Expression of four mitochondrial tRNAs from only two loci

Jessica M. Warren[1,2], Kasavajhala V.S.K Prasad[3], Anistynn M. Mendez[1], Stephanie Temnyk[1], John P. McCutcheon [1,2]

[1] Biodesign Institute and School of Life Sciences, Arizona State University, Tempe, Arizona, United States of America
[2] Howard Hughes Medical Institute, Chevy Chase, Maryland, United States of America
[3] Department of Biology, Colorado State University, Fort Collins, Colorado, USA
Jessica M. Warren[1]
Email: Jessica.M.Warren@asu.edu

Abstract

Transfer RNAs (tRNAs) are among the few genes retained in animal mitochondrial genomes after more than a billion years of gene loss. These ancient bacterial vestiges are often structurally aberrant and less stable than their bacterial or cytosolic tRNA counterparts. In some lineages, mitochondrial tRNAs (mt-tRNAs) have become so truncated that the loss of one or both arms has expanded our understanding of what constitutes a functional tRNA. Here, we report another radical departure from canonical tRNA gene architecture: two overlapping tRNAs produced from opposite strands of the same locus. These 'mirror' tRNA pairs eliminate the need to retain separate loci for all tRNA genes, as a single locus can produce tRNAs to decode two different amino acids. We show that these mirror tRNAs are aminoacylated and demonstrate their presence in mitoribosomes. Furthermore, mirror tRNAs display strand-specific patterns of nucleotide modification and RNA editing, reflecting specific post-transcriptional maturation that depends on transcriptional orientation. To our knowledge, this demonstration of functional, bidirectional tRNA expression is a first for any genome or organism and reveals an unexpected strategy by which mitochondrial genomes maintain a complete set of tRNAs in the face of unrelenting gene loss. The discovery of mirror tRNAs has broad implications for the evolution of tRNA-interacting enzymes, mitochondrial biology, and even the origins of the protein synthesis machinery itself.

Significance Statement

Mitochondrial genomes have been reduced to only a handful of genes over the roughly two billion years since the origin of the organelle. Despite this extreme gene loss, bilaterian animal mitochondrial genomes still retain a complete, minimal set of tRNAs necessary for protein synthesis. Here, we identify a previously unrecognized strategy in animal mitochondria to maintain a complete set of tRNAs – the bidirectional expression of a single genomic locus to produce two different tRNAs. These "mirror" tRNAs are aminoacylated, incorporated into mitoribosomes, and exhibit strand-specific patterns of editing and modification. This surprising coding strategy reveals how mitochondrial genomes can preserve a complete set of tRNAs despite unrelenting gene loss.

Main Text

Introduction

The mitochondrial genomes of most bilaterian animals have been reduced to a remarkably conserved set of the same 37 genes, 22 of which encode transfer RNAs (1). These 22 mitochondrial tRNAs (mt-tRNAs) are considered a minimally sufficient set of tRNAs to decode all 60 codons for the 20 amino acids in the mitochondrial genetic code (2). This almost one-to-one relationship between amino acids and tRNAs is in striking contrast to the more than 50 species of tRNAs used for decoding all codons in prokaryotic or eukaryotic cytosolic translation and represents a fascinating example of a near-minimal protein synthesis system (3). However, this stubborn retention of mt-tRNAs in animals is not universal in mitochondrial evolution. The mitochondrial genomes (mitogenomes) of most non-animal eukaryotes have lost tRNAs beyond this minimal set and rely on the import of nuclear-encoded tRNAs to maintain mitochondrial translation (4, 5). Therefore, encoding a full set of native mt-tRNAs, once thought to be the general rule, actually represents an exceptional case of genetic entrenchment.

This conservation of tRNAs on the animal mitogenome has had profound consequences for the structural evolution of mt-tRNAs. Bilaterian mitogenomes experience a much higher rate of sequence evolution than the nuclear genome due to their high mutation rates, asexual reproduction, limited recombination, and frequent population bottlenecks (6). Over 500 million

years of animal evolution, the accumulation of slightly deleterious mutations has resulted in animal mt-tRNAs being shorter and having overall less thermal stability than their nuclear counterparts(7–9). tRNA truncation has been so extensive in some lineages that numerous mt-tRNAs have lost the entire D- or T-arm, and in the most extreme cases, both arms have been lost and the mt-tRNA is now just a simple stem-loop structure (10–12).

Here, we report a new way in which mt-tRNA evolution has pushed the bounds of genetic compaction. We show that in the mitochondrion of the citrus mealybug (*Planococcus citri*), four functional tRNAs are produced from two tRNA loci, and that the expression, modification, and aminoacylation of these four tRNAs provides *P. citri* mitochondria with its complete set of 22 mt-tRNAs from only 20 mt-tRNA loci.

Results

The *P. citri* mitogenome is the expected size for an animal but is extremely A/T biased

A previous *P. citri* mitogenome has been published (GenBank: OX465514) as part of the Wellcome Sanger Tree of Life Programme. However, we noticed that this genome was almost twice the size (at 30,900 bp) of other assembled Coccoidea (scale insects) mitogenomes, including the closely related *Phenacoccus manihoti* (14,965 bp). The published *P. citri* mitogenome assembly also appears to contain a large, inverted duplication. We suspected that these features were due to misassembly errors. We therefore re-sequenced and re-assembled the *P. citri* mitogenome using Oxford Nanopore on isolated mitochondrial DNA. This new assembly resulted in a 14,910 bp circular molecule that shares 98.8% sequence identity with the previously published mitogenome and has been deposited in Genbank (Supp. File 1). The overall base pair composition of the mitogenome is extremely A/T biased with 90.8% A/T (9.2% G/C) and contains a control region with a large “ATAT” tandem duplication.

Multiple *P. citri* protein-coding genes are not predicted to be in continuous open reading frames but are transcribed and translated into proteins

Annotation of the protein-coding genes in the *P. citri* mitogenome was done using sequence similarity searches to the *P. manihoti* mitochondrial proteins. We found a region of the *P. citri* genome with significant similarity to all 13 protein-coding genes typically found in animal mitogenomes (Fig.1A). Nine of the protein coding genes (ATP6, ATP8, COX2, COX3, CYTB, ND2, ND3, ND6, and ND4L) had continuous open reading frames (ORFs) bounded by canonical start/stop codons as found in other invertebrate mitogenomes (Supp. Fig. 1). However, the remaining four genes (COX1, ND1, ND4, and ND5) did not occur in the genome as continuous ORFs. Instead, these genes have multiple coding regions with similarity to a *P. manihoti* gene. These sequences were either found with fragments in multiple reading frames or contained premature stop codons if translated in a single frame (Supp. Fig. 1).

To test whether these discontinuous gene hits were an artifact of sequencing/assembly errors or were truly reflected in the mRNAs, we performed full-length mRNA sequencing (IsoSeq) and mapped these reads to the *P. citri* mitogenome (Supp. Fig. 1). Mapped IsoSeq reads matched the reading frames of the mitogenome assembly, ruling out genome assembly errors. ORFs generated from IsoSeq reads followed the same pattern as the mitogenome search, resulting in nine protein coding genes existing in a single frame, and four others being fragmented in multiple ORFs.

The finding of discontinuous ORFs for these protein-coding gene raises multiple possibilities. The genes could be pseudogenes, although it would be extraordinary to lose these respiration-related genes in an aerobic mitochondrion (13). Alternatively, codon reassignment,

ribosomal frameshifting, transcriptional slippage, or true gene fragmentation and assembly have all been reported in mitochondria and could also be occurring in *P. citri* to restore full-length proteins/complexes. We searched the regions suspected to have frameshifts for any common codon and/or sequence patterns that could serve as translational exceptions and failed to find any exact motif at all suspected frameshifts. There was, however, a homopolymer of As or Ts of various lengths in the predicted frameshift regions for multiple genes. Both the ORFS for each gene as well as the predicted frameshift positions have been annotated in Supp. Table 1.

Finally, we performed tandem mass spectrometry (MS/MS) on purified mitochondrial proteins and detected peptides from COX2, COX3, CYTB, ND3, the first ORF of ND1, the second ORF of COX1, and the second ORF of NAD4 (Supp. Table 2). These data demonstrate that both proteins encoded on a single continuous frame and those with multiple ORFs are being translated into proteins and suggests that none of the expected 13 protein coding genes are functionally missing from the mitogenome despite some genes not being encoded in canonical or single ORFs.

The *P. citri* mitogenome contains tRNA genes undetectable by tRNA search programs but identifiable from full-length tRNA sequencing

We scanned the *P. citri* mitogenome with tRNAscan-SE (14) which resulted in only two tRNA predictions (tRNA-Ile and tRNA-Leu(TAA)). Using the mitochondrial-specific annotation tool MITOS2 (15) resulted in 17 predicted tRNAs but with multiple predictions having poor e-value scores. Combined, these computational approaches found no putative tRNA-Ala, tRNA-Gln, tRNA-Leu(TAG), tRNA-Tyr, or tRNA-Val (Supp. Table 3), possibly due to the extreme A/T bias of the mitogenome and/or degenerate tRNA structure of the putatively encoded tRNAs.

In order to identify tRNAs not predicted using computational approaches and find the exact genomic start/stop coordinates of each tRNA, we performed full-length tRNA sequencing using YAMAT-seq (16) on total RNA isolated from gradient-purified *P. citri* mitochondria (Fig. 1A). YAMAT-seq uses splint-assisted ligation with adapters that complement the CCA overhang found on all mature tRNAs (16). Read abundances from YAMAT-seq libraries can be highly biased due to inefficient reverse transcription of some tRNAs due to base modifications (17). However, because both adaptors are ligated directly to mature tRNAs during library preparation, full-length tRNA sequences are amplified during sequencing library creation and can be used to determine tRNA gene bounds.

YAMAT-seq libraries from purified *P. citri* mitochondria resulted in 23 clear 'hotspots' in the mitogenome corresponding to region with a large percentage of mapped reads (Fig. 1A). From these regions with abundant YAMAT reads, 23 candidate tRNA sequences were identified, and the most frequent first and last positions for each sequencing peak were assigned as the gene's boundaries.

All 17 of the MITOS2 predicted tRNAs corresponded to a hotspot region with high read abundance (Supp. Table 3). For 16/17 of those tRNAs, the most abundant start/stop read coordinates were within 4 bp of the computationally predicted start/stop coordinates (Supp. Table 3). Only tRNA-Arg was substantially different than the predicted sequence at 10 bp shorter. Although tRNA-Gln, tRNA-Leu(TAG), and tRNA-Tyr were not identified in the mitogenome when using computational approaches, we found a highly expressed region of the mitogenome that contained the corresponding anticodon to each of these missing tRNAs (Fig.1B, Supp. Table 3). These sequences were BLASTed to mt-tRNA databases from close relatives (Supp. Table 3) to test for sequence similarity to other mt-tRNAs. By taking a combination of the best hit in conjunction with RNA folding strategies (see section on tRNA structure below) the tRNA-Gln, tRNA-Leu(TAG) and tRNA-Tyr were identified and annotated (Fig. 1B).

The mitogenome encodes multiple tRNA 'mirrors', tRNAs produced from opposite strands of a single genomic location

Surprisingly, three genomic locations with a putative tRNA gene had substantial YAMAT expression from both strands, and both orientations were post-transcriptionally modified with a CCA tail (Fig. 2, Supp. Table 3). These mirrored tRNAs carry reverse-complement anticodons: tRNA-Cys(GCA) mirrors tRNA-Ala(TGC), and tRNA-Tyr(GTA) mirrors tRNA-Val(TAC) (Fig. 3) Two of these mirrored tRNAs, tRNA-Ala(TGC) and tRNA-Val(TAC), contain the two anticodons missing from the rest of the predicted tRNA set. As the expected 22 mt-tRNAs can only be accounted for by including the bidirectional expression of these two tRNA loci (tRNA-Tyr/Val and tRNA-Cys/Ala), these data raise the possibility that a single tRNA locus is being transcribed to produce two distinct tRNAs, one from each strand. The tRNA-Pro(TGG) locus also had substantial antisense expression (designated as trnX, Fig. 2), but a tRNA with the anticodon CCA (decoding tryptophan) is not typically found in animal mitochondria (18), making the function of this transcript unknown. All other genomic locations with a computationally or experimentally predicted tRNA gene only had appreciable sequence coverage arising from one strand of the genome (Fig. 2).

Although very rare in bilaterian animals, mt-tRNA gene loss and functional replacement through the import of nuclear-encoded tRNAs does occur in many other eukaryotic lineages (5, 19). To test for the possibility that *P. citri* has functionally lost mt-tRNAs and is now importing nuclear-encoded tRNAs, we performed differential abundance analysis on gradient-purified mitochondrial samples vs. total insect samples to assess if any tRNAs not encoded on the mitogenome were enriched in *P. citri* mitochondria. A database of all *P. citri* nuclear, mitochondrial, and bacterial endosymbiont tRNAs (*P. citri* has two nutritional endosymbionts encoding their own tRNAs) was assembled (Supp. Table 4), and YAMAT libraries were sequenced from three total insect and gradient-purified mitochondria samples and mapped to this database (all mapped counts for all YAMAT-seq libraries in Supp. Table 5). As expected, all the mitochondrial tRNAs were highly enriched (>19 fold) in mitochondrial fractions; however, no nuclear tRNAs approached that enrichment level in the analysis (Supp. Fig. 2, Supp. Table 6). The failure to identify strong candidates for preferential import of any nuclear-encoded tRNAs suggests that *P. citri* mitochondria still rely on natively encoded mt-tRNAs for translation despite the extremely degenerate nature of the mt-tRNAs.

***P. citri* mt-tRNAs are the most A/T biased tRNAs reported**

With an average length of only 58 bp, the majority (15/22) of the mt-tRNAs are too short to produce a canonical cloverleaf tRNA shape with both D- and T-arms (Fig. 4, see Supp. Fig. 3 for all mt-tRNA models). The truncated and extreme A/T bias of these tRNAs prevents RNA folding algorithms such as RNAfold (20) from predicting the expected stem and loop structures found in tRNAs; therefore, we manually folded all tRNA sequences to maintain these features (Fig. 4 and Supp. Fig. 3). Although many of the tRNAs are represented as missing only one arm (retaining either a D- or T-arm), these stems were often short (> 4 bp) and sometimes contained modified bases that would interfere with base pairing (see section on base modification below), raising the possibility that some of these tRNAs may actually be armless *in vivo*. The A/T composition of the tRNAs is extraordinarily biased, with a range of 82-96% A/T and an average of 90.6% A/T (Table 1, Supp. Table 3). Remarkably, tRNA-Leu(TAG) is almost 97% A/Ts, having only 1 G and 1 C that are not part of the non-templated CCA tail, and lacks even a single C-G base pair (Fig. 4).

Table 1. A/T nucleotide composition across diverse A/T-biased genomes. Shown are overall A/T percentages for genomes, protein-coding sequences, and tRNA genes from mitochondrial, plastid, apicoplast, and bacterial endosymbiont genomes.

Species	Organism	Genome	Accession	Overall A/T %	Protein coding A/T %	tRNA A/T %
Planococcus citri	**Insect**	**Mitogenome**	**This study**	**90.9**	**88.9**	**90.6**
Phenacoccus manihoti	Insect	Mitogenome	NC_066716	89.3	88.8	86.1
Drosophila melanogaster	Insect	Mitogenome	KJ947872	82.2	77.2	77.1
Tetranychus urticae	Arachnid	Mitogenome	NC_010526	84.3	84.0	84.1
Ulva prolifera	Green algae (Chlorophyta)	Plastid	NC_036137	75.2	74.5	48.0
Balanophora laxiflora	Flowering plant	Plastid	KX784265	87.8	91.1	70.7*
Plasmodium falciparum	Apicomplexan	Apicoplast	LR605956	85.8	89.1	73.3
Shikimatogenerans sp. Tmey	Bacterial endosymbiont (Flavobacteriales)	Endosymbiont	CP146597	87.9	88.2	61.3
Zinderia insecticola	Bacterial endosymbiont (Burkholderiales)	Endosymbiont	CP002161	86.5	86.8	55.8

* The *B. laxiflora* plastid encodes a single tRNA gene (tRNA-Glu).

Mirror mt-tRNAs expressed from opposite strands have unique modification and editing profiles

All tRNAs typically have multiple modified nucleotides (21, 22), and these modifications can play critical roles in tRNA structure and function. Because some base modifications can inhibit reverse transcriptase (RT) activity, modifications can be mapped to specific nucleotides in a tRNA through the detection of RNA polymerase errors (nucleotide misincorporations and indels) in the resulting cDNA (23–25). These misincorporation signatures can then be used to infer both the position and the identity of the modification, producing a modification map or 'index' of a tRNA. We applied a modification detection pipeline to the *P. citri* mt-tRNAs to produce a tRNA modification index by globally aligning mapped reads to each reference using MAFFT (26) and calculating percentage of mismatched reads for each position along the tRNA (see Supp. Table 7 for all aligned base calls).

The number of detected modifications for the mt-tRNAs was low, with an average of only 1.87 detected base modifications per tRNA when a 20% cDNA misincorporation threshold was applied. There was, however, a consistent signal of a base modification in 5' region of the mt-tRNAs (Fig. 4, Supp. Fig. 4). All but one mt-tRNA had evidence of one or multiple A or G modifications within positions at 7-9 of the tRNA (Supp. Fig. 4). One likely candidate is 1-methyladenosine (m^1A) which is a very common base modification in mt-tRNAs and is known to cause RT-inhibition signatures (27). Only three mt-tRNAs (Cys, Phe, and Tyr) had RT-inhibiting base modifications in the anticodon loop, and in all cases, the misincorporation signal was a two base pair deletion immediately following the anticodon. The modifications N6-

isopentenyladenosine (i^6A), or the modified i^6A, 2-methylthio-N6-isopentenyladenosine (ms^2i^6A), are known to occur on animal Cys, Phe, and Tyr mt-tRNAs at this position (27), and their bulky nature often cause reverse transcriptase stalling/skipping instead of misincorporating the wrong nucleotide (28).

Notably, the two pairs of mirrored tRNAs (Ala/Cys, and Tyr/Val) have very different predicted secondary structures and entirely different modification profiles from their complementary sequence (Fig. 2). Mt-tRNA-Ala has evidence of a base modification at position 8A, whereas its tRNA-Cys mirror lacks a modification at any position in the 5' region, and instead has the bulky modification immediately following the anticodon mentioned previously. Mt-tRNA-Tyr is the most modified mt-tRNA in these data, with five different modifications (Fig. 2, Supp. Fig. 3) whereas its mirror tRNA-Val lacked a strong signal for base modification at any position (Fig. 2).

In addition to base modifications, mt-tRNAs can also have bases added post-transcriptionally to produce a final sequence that is different than the sequence in the mitogenome. One example that has been reported in multiple animals is the addition of adenosine at the 3′-end of mt-tRNAs prior to CCA tailing (29). This type of editing often occurs when partially overlapping tRNA genes produce truncated sequences that are then post-transcriptionally “finished” to restore a full-length tRNA. In *P. citri*, mt-tRNA-Gln, Gly, Met, Thr, and Val all had the addition of a single adenosine at the 3′-end, and the tRNA-Ala had the addition of two adenosines (Supp. Table 2).

Mirror mt-tRNAs expressed from opposite strands are aminoacylated

For a tRNA to be functional in translation it must first be aminoacylated, or “charged,” with an amino acid to the terminal adenosine in the CCA tail. Charged tRNAs can be quantified using recently developed tRNA sequencing methods that use the Whitfeld reaction to remove the terminal 3′ nucleotide of uncharged tRNAs that lack the protective amino acid (30, 31). The percentage of reads ending in a CC (not aminoacylated) vs those ending in the complete CCA (aminoacylated) can then be used to measure the proportion of aminoacylated molecules for a specific tRNA (Fig. 4A). We used this method to determine which of the identified sequences in the *P. citri* mitochondria could function in translation and test whether both mirror tRNAs produced from a single locus were aminoacylated.

Three biological replicates from gradient-purified *P. citri* mitochondria were used to generate and sequence multiplex small RNA-seq (MSR-seq) libraries (30). Each replicate was split into two subsamples where one subsample was treated with periodate to distinguish between aminoacylated and uncharged tRNAs, and the other served as a negative control with no periodate treatment. This negative control provides insight into the base level of CCA tailing and any CCA tail damage during extraction. The average percentage of CCA reads in these untreated libraries was approximately 74% for the mt-tRNAs (Fig. 4B, Supp. Table 8). A synthetic Bacillus tRNA-Ile(GAT) served as an uncharged tRNA control and was added to all samples after RNA extraction, but before the beginning of library preparations to measure the effectiveness of periodate treatment in removing the terminal A nucleotide.

One difficulty in applying these aminoacylation detection methods to the *P. citri* mt-tRNAs was the extreme A/T bias and the necessary number of PCR cycles used to amplify MSR-seq libraries. PCR and Illumina sequencing have known biases against A/T rich sequences, resulting in lowered or even elimination of A/T biased sequences in the final read population of complex libraries (32). When applying 15 cycles of PCR, periodate treated libraries had pronounced drop out of the most A/T rich sequences and those mt-tRNAs expected to have the lowest expression (Supp. Fig. 5). However, when lowering the number of PCR cycles to 10 or 6 cycles and using a barcoding and library pooling scheme, we were able to detect all 23 mt-tRNA references in treated and untreated libraries (Supp. Fig. 5).

Periodate treatment was very effective at removing the terminal A in the uncharged tRNA spike-in control, with an average of only 2% of the reads ending in the complete CCA in the treated libraries (Fig. 4B). In contrast, the average percentage of mt-tRNA reads ending in CCA was 34.2% (Fig. 4B, Supp. Table 8B). Across all mt-tRNAs, periodate treatment revealed a strong and highly significant protection relative to the uncharged Bacillus spike-in (FDR $\ll$ 0.05, binomial glm), with odds ratios ranging from 21-fold (tRNA-Cys) to greater than 400-fold (tRNA-Val) (Supp. Table 8C). Mt-tRNA-Cys and mt-tRNA-Ala had the fewest reads mapped, resulting in high standard deviation of the read classes. However, the average percentage of reads with the complete CCA tail for both mt-tRNA-Cys and mt-tRNA-Ala was still much higher than the negative control with 25.5% and 19.0%, respectively (Fig. 4). The detection of mt-tRNA-Tyr and mt-tRNA-Val sequences was marginally better and had higher-than-average CCA read percentages with 48.7% and 53.2%, respectively. The antisense expression of tRNA-Pro (trnX) was an interesting case, because although this sequence was statistically more protected than the uncharged spike-in (Supp. Table 8C), it still showed very little retention of the complete CCA tail, with an average of 5.6% of the reads containing the terminal A across the replicate libraries. This low rate of protection provides evidence that this RNA is not significantly aminoacylated and may not be participating extensively in translation as a true tRNA.

We also calculated the percentage of reads ending in CCA for nuclear tRNAs in these libraries (Supp. Fig. 6) and found an overall average of 37%. The average percentage of reads ending in CCA for all *P. citri* tRNA references can be found in Supp. Table 8. Overall, these data support the hypothesis that *P. citri* maintains 22 aminoacylated mt-tRNAs.

Mirror mt-tRNAs are found in mitochondrial ribosome isolates, with mt-tRNA-Val found in very high abundance.

To test the occupancy of mt-tRNAs in the mitochondrial ribosome, we performed mitoribosome tRNA-seq by isolating mitochondrial ribosomes through sucrose density gradient centrifugation followed by YAMAT-seq on RNA isolated from those fractions. While raw abundance values from tRNA sequencing methods likely do not reflect absolute biological abundances due to reverse transcription stalling from tRNA modifications, relative comparisons across samples and treatments using the same tRNA-seq method can provide meaningful abundance differences. Using this logic, we next measured whether the tRNA population in whole mitochondria was different than the tRNA population purified with mitoribosomes, if these differences reflected amino acid demand, and if the mirror tRNAs were abundant in mitochondrial ribosome fractions.

Mitoribosomes are substantially smaller than cytosolic ribosomes and can be separated based on differences in sedimentation (33). We separated *P. citri* mitoribosomes from cytosolic ribosomes using differential centrifugation followed by sucrose gradient fractionation (Fig. 5A). Gradients were fractionated while monitoring absorbance at 260 nm to identify ribosome-containing fractions. The absorbance profile showed multiple peaks, including a distinct peak preceding the large cytosolic ribosome peak (Fig. 5A). To verify ribosome separation, total RNA was extracted from each fraction and RT–qPCR was performed targeting the large rRNA from each ribosome class (primers can be found in Supp. Table 9). Mitochondrial rRNA was most abundant in fractions 6–7 (Supp. Fig. 7). RNA from fractions 6–8 was therefore pooled for mitoribosome tRNA sequencing.

With an average of 88.9% of the reads from the mitoribosomes libraries mapping to a mt-tRNA reference, these mitoribosome tRNA-seq libraries were highly enriched for mt-tRNAs compared to whole insect, or even when compared to gradient-purified mitochondria libraries (Fig. 5B). The relative abundance of each mt-tRNA changed considerably in isolated (total) mitochondria libraries compared to mitoribosome libraries. Most notably, there was an extreme abundance of reads mapping to mt-tRNA-Val in mitoribosome samples, representing an average of 38.8% of the reads (Fig. 5B). As animal mitochondrial ribosomes have been reported to use mt-tRNA-Val as a structural component of the ribosome itself (replacing the 5S rRNA) (34), this

high abundance of mt-tRNA-Val may reflect its role as a structural component of the mealybug mitoribosome.

To test whether mitoribosome tRNA-seq abundances reflect amino acid usage in the mitochondrial proteome, we computed Hedges' g (a small-sample size corrected Cohen's d) for each tRNA using CPM-normalized read counts and comparing mitoribosome to total mitochondrial read abundances. We then regressed this mean difference statistic (Hedges' g) on the frequency of the cognate amino acid in the mitochondrial proteome (Fig. 5C). This was done under the premise that the standing tRNA population in whole mitochondria would be different than the population loaded in the mitoribosomes, and that this difference should reflect amino acid demand. Association strength was evaluated by simple linear regression (g ~ amino-acid frequency) and found to have a Pearson r correlation of 0.65 ($p = 0.00108$) and Spearman correlation coefficient of 0.63 ($p = 0.00133$), representing a moderately strong relationship between tRNA-seq abundance in the mitoribosome samples and amino acid use. The mitochondrial proteome in *P. citri* is extremely biased as a consequence of the extreme A/T composition of the genome. Only five amino acids (Ile, Leu, Phe, Asn, and Met) make up over 68% of the amino acids in the proteins encoded on the mitogenome, and the tRNAs that carry these amino acids had a much greater change of abundance in the mitoribosome samples than the other tRNAs (Fig. 5C). 13/22 mt-tRNAs were within a 95% confidence interval (CI) of expected mitoribosome occupancy (Fig. 5C). The amino acids Ala and Cys are the least common amino acids in the mitochondrial proteome (representing 0.57% and 0.37% respectively), but both tRNAs originating from the tRNA-Cys/Ala locus were found to be in the CI of expected abundance change in mitoribosome samples. In contrast to the extreme overrepresentation of mt-tRNA-Val, the mirrored sequence at this locus, tRNA-Tyr, was solidly in the CI of expected abundance change in mitoribosome samples (Fig. 5C).

Discussion

The complementary expression of two tRNAs from a single locus is a major departure from the known tRNA gene organization of all types of genomes and organisms. There are rare examples of two proteins being encoded with bidirectional expression of a locus producing two different proteins (35, 36), but the majority of functional antisense gene expression is the generation of a noncoding RNA complementary to mRNA with modulating effects on its translation (37, 38). The complementary nature of DNA/RNA double strands and the stem-loop, palindromic structure of tRNAs may make them amenable to this unusual form of mirrored expression.

Antisense expression is ubiquitous in animal mitogenomes, as both strands are fully transcribed and later processed by RNA maturation enzymes to release individual RNAs from the polycistronic precursor (39).Typically, these transcriptional byproducts are rapidly degraded and maintained a very low level (40, 41). Nevertheless, the origin of mirror tRNAs could evolve in a straightforward manner, where a spurious, antisense transcript of a tRNA has enough structural similarities to be recognized by tRNA maturation enzymes and processed like a bona fide tRNA, thereby avoiding the degradation pathway. For example, the CCA-adding enzyme has been shown to act on non-tRNA substrates that have a stem-loop structure (42, 43). If these processed sequences can then be recognized by an aaRS, the result would be a pool of aminoacylated mirror tRNAs alongside the ancestral mt-tRNA. The participation of these mirror tRNAs in ribosomal decoding would effectively make the ancestral tRNA gene redundant, eventually allowing for its eventual loss and making the system functionally dependent on the bidirectional expression of one tRNA locus.

The presence of small (1-3 bp) overlaps in mt-tRNA genes is common in animal mitogenomes (44). These overlaps often result from truncated acceptor stems which are then

repaired through the post-transcriptional addition of 3' nucleotides (29, 45–47). An extreme situation of mt-tRNA gene overlap has been suggested for the isopod *Armadillidium vulgare* where the mt-RNA-Cys and mt-tRNA-Tyr genes are predicted to overlap by 20 bp on the same strand, and the mt-tRNA-His and mt-tRNA-Phe genes are predicted to overlap by 19 bp on the opposite strand (48). The sequencing of RT-PCR products from the mt-tRNA-His confirmed the presence of a CCA tail in addition to extensive 3' editing of nucleotide additions not encoded in the mitogenome (48). Importantly, though, no full-length tRNA sequencing has been performed to confirm the coordinates of the potentially overlapping genes. A fascinating possibility is that mirrored expression of mt-tRNA genes in *A. vulgare* eliminates the need to postulate gene overlap for some of the mt-tRNAs. Notably, *A. vulgare* has an interesting situation where the mt-tRNA-Val and mt-tRNA-Cys genes occur in a heteroplasmic state whereby only a proportion of mitogenomes encode either of those two tRNAs at the same relative genomic location (49). Given that both tRNAs are mirrors in *P. citri*, it raises the possibility that this locus in *A. vulgare* is producing four separate tRNAs instead of just two. There is even evidence that the antisense transcription of this heteroplasmic locus is being recognized by tRNA-processing enzymes (48).

Regardless of whether mt-tRNA gene overlap is frequently occurring at only a few base pairs followed by repair or at a larger scale, it is difficult to imagine a scenario whereby tRNA mirrored expression could evolve through a "creeping overlap" mechanism. Notably, although some *P. citri* mt-tRNAs are being edited though the addition of 1-2 non-templated As (Supp. Table 3), the mirror tRNAs we report here do not arise from truncated transcripts which are then edited to full-length tRNAs: they are encoded on the genome as overlapping tRNA genes which share completely overlapping anticodons (Fig. 2). We suspect that the centering of both tRNAs around the same genomic location would have been nearly impossible through a progressive shift of transcription. Instead, the wholesale bidirectional expression of a single locus followed by slightly different cleavage points from the polycistronic transcript would give rise to two tRNAs that have mirrored anticodons.

Determining the identity of the ancestral (and lost) mt-tRNA genes in *P. citri* was complicated by the truncated and incredibly A/T biased nature of the sequences. This difficulty was particularly true for the mt-tRNA-Cys/Ala locus. For consistency, we used the MITOS2 call for the identification of the ancestral tRNA at this mirror position, but the score was quite low (Supp. Table 2). There is, however, evidence from gene synteny that this locus was ancestrally tRNA-Ala in scale insects (Fig.1B). Additionally, insects have a conserved 3G-C70 base pair in mt-tRNA-Ala (48), which is present in the *P. citri* sequence (position 3G-57C, Supp. Fig. 4) and this G-C base pair would not exist in antisense expression of the ancestral mt-tRNA-Cys. For tRNA-Val/Tyr mirrors, there was not strong syntenic evidence for the identity of the tRNA at this position (Fig.1B), but this sequence showed significant similarity to previously annotated tRNA-Tyr in multiple scale relatives (Supp. Table 3). The high abundance of this tRNA in the mitoribosomes fractions suggests that mt-tRNA-Val is a structural component of the mitoribosomes like in mammals (50). If true, that would mean that the mirrored expression of the mt-tRNA-Tyr gene has replaced both the mt-tRNA-Val in decoding as well as a structural component of the mitoribosome.

The widespread antisense/mirror expression and CCA-tailing of mt-tRNA genes was first reported in the unrelated spider mite *Tetranychus urticae*, where nine mt-tRNAs were found to have substantial anti-sense expression and posttranscriptional modification (12). However, the mitogenome of *T. urticae* still encodes the expected 22 mt-tRNA genes, making the complementary expression of mt-tRNAs redundant (all the anticodons are still encoded by a separate tRNA gene) and thus the functional significance of these mirrors unknown. It would be interesting to determine if these anti-sense tRNAs are aminoacylated in *T. urticae* as this species may represent an intermediate evolutionary step prior to the loss of one of the mt-tRNA genes as reported in *P. citri*.

Notably, *T. urticae* mt-tRNAs are also truncated and A/T rich like that of *P. citri*. In fact, multiple animal lineages have independently evolved short mt-tRNAs structures (44). In addition to multiple arachnid lineages of spiders and mites (11, 51–53), a class of nematodes (Enoplea) has also been reported to have highly degenerate mt-tRNA structures (54, 55). The mitogenome of the nematode *Romanomermis iyengari* has some of the shortest tRNAs reported and is actually annotated as having mirror Ala/Cys mt-tRNAs (10). However, subsequent computational searches in Enoplea mitogenomes found 22 separate mt-tRNA candidate genes without needing to postulate the existence of mirrors (10). Difficulty in predicting degenerate mt-tRNAs has resulted in numerous annotations missing mt-tRNA genes below the expected 22 and highlights the importance of generating experimental evidence for these essential gene products. But the functional expression of mirrored mt-tRNAs in *P. citri* and the presence of antisense/mirror tRNA sequences in the unrelated mite *T. urticae* raises the fascinating possibility that tRNA mirroring is an evolutionary route for mt-tRNA gene loss and may have convergently evolved multiple times independently.

The theoretical existence of mirror mt-tRNAs has been proposed both in extant systems (56) and in the ancestral decoding apparatus of early life (57, 58).The Rodin and Ohno hypothesis proposes that the two major classes of aminoacyl-tRNA synthetases (Class I and II) originated from complementary strands of a common ancestral gene, and that these enzymes charged mirror tRNA molecules. Rodin and Ohno highlight the striking structural symmetry that Class I and Class II aaRSs interact with opposite grooves of the tRNA acceptor stem, and the codons they recognize correspond to complementary tRNA anticodon triplets, dividing the genetic code along a strand-symmetric axis (57). The discovery that mirror tRNAs have evolved in a bilaterian animal mitogenome that experiences strong genetic drift and a high substitution rate may offer insight into the limits of a minimal translation system and a window into the ancient and ancestral core translation machinery. As drift becomes a greater force in the evolution of genomes, only the most deleterious mutations are selected against (59). This process may eventually lead to mutational meltdown (60) but may also result in the winnowing of a system down to its most essential components (61). Therefore, the reduction in the number of tRNA loci and the bidirectional expression of mt-tRNA in *P. citri* may represent an extreme form of system reduction akin to the ancestral decoding system. Evidence for reductive processes being used as windows into ancestral machinery may also be found in the reduced mt-tRNA structures themselves. The loss of both arms in mt-tRNAs in multiple lineages (including possibly *P. citri*) shares resemblance to the minihelix, a simple stem-loop structure proposed to be the ancestral tRNA molecule (62, 63).

Finally, the mirrored expression of tRNAs poses a striking evolutionary problem for *P. citri*: how do tRNA-interacting enzymes adapt to substrates transcribed from both strands? Because tRNAs and aaRSs are typically tightly co-evolved to ensure the faithful decoding of the genome, the existence of mirror tRNAs implies that a single genomic locus must maintain compatibility with two distinct aaRSs acting on complementary substrates. Genes predicted to encode separate mitochondrial Cys, Ala, Tyr, and Val aaRSs are present in the *P. citri* nuclear genome (Supp. Table 10), but it remains unclear how these enzymes accommodate the mirrored tRNA structures, or whether distinct structural adaptations have evolved to recognize them.

Methods

Crude isolation of *P. citri* mitochondria

Mealybugs were reared on small potatoes in a chamber set to 12 hr light/ 12 hr dark at 26°C with 50% relative humidity. About 2 g (~10,000 individuals) of mealybugs at all life stages were used

for each mitochondrial isolation. Mealybugs were removed from the potatoes, washed in 70% EtOH, and then washed again in isolation buffer (50mM HEPES-KOH pH7.5, 10mM KCl, 1.5mM MgOAc, 70mM sucrose, 210mM mannitol, 1mM EDTA, 1mM EGTA, 1mM DTT). Cleaned mealybugs were added to a 7 mL glass dounce homogenizer with 4 mL fresh isolation buffer and dounced 10x times with the loose pestle and 10X times with the tight pestle. The homogenate was filtered over 4 layers of pre-wet cheese cloth and one layer of Miracloth over a funnel, making sure to squeeze as much liquid out as possible. Filtered homogenate was spun at 1,000 g for 5 min at 4 °C with a fixed angle rotor (Beckman Ti 90). Pellet was discarded and supernatant was spun again at 1,000g for 5 min at 4 °C. Pellet was again discarded, and the supernatant was filtered over a 100 µm mesh filter. To remove any residual wax, the supernatant was again filtered over a fresh 100 µm mesh filter. Cleaned supernatant was spun at 15,000g for 15 min at 4 °C to pellet mitochondria. The supernatant was discarded, and the crude mitochondria pellet was resuspended into 1 mL SEM buffer (250mM sucrose, 20mM HEPES-KOH pH7.5, 1mM EDTA, 1mM EGTA) with a paint brush. This crude mitochondrial isolate went directly into sucrose gradient purification (see below), or the pellet was snap frozen in liquid nitrogen for use in mitochondrial ribosome isolations or DNA extractions.

Gradient purification *P. citri* mitochondria

Resuspended crude mitochondrial pellet was transferred to a 2 mL glass dounce and dounced 4x times with the loose pestle. This suspension was carefully layered on top of a 15-23-32-60% sucrose gradient (in 50mM HEPES-KOH pH7.5, 1 mM EDTA, 1mM EGTA) in a swinging bucket rotor (Beckman Ti 40). The gradient was spun at 28,000g for 1 hr at 4 °C. Purified mitochondria formed a band at the 32/60% interface and was collected by aspiration. Purified mitochondria were washed by adding 5X volumes of SEM buffer and spun at 15,000g for 15 min. Supernatant was discarded and the pellet was snap frozen in liquid nitrogen for further analyses.

***P. citri* mitogenome sequencing and assembly**

Nanopore sequencing: High molecular weight DNA was extracted from a crude mitochondrial isolation and sequenced with Oxford Nanopore, using the Ligation Sequencing Kit (SQK-NBD114.24) with the NEBNext Companion Module (E7180L) to manufacturer's specifications. Guppy1 (v6.5.7) was used for basecalling (SUP), demultiplexing, and adapter removal. Reads were trimmed with Porechop (0.2.3-seqan2.1, (--discard_middle).

Illumina sequencing: DNA was extracted from a crude mitochondrial isolation and sequenced with the NovaSeq X Plus sequencer with 2x151bp paired-end reads. Illumina sequencing libraries were prepared using the tagmentation-based and PCR-based Illumina DNA Prep kit. PCR amplification was done with only 5 cycles of PCR. Library was sequenced on Demultiplexing, quality control was performed with bcl-convert1 (v4.2.4). Reads were trimmed with cutadapt (-q 20 --minimum-length 50 -e 0.15 -j 24).

Assembly: Trimmed Nanopore reads were BLASTed (blastn -dust no -evalue 1e-7) to the previously published P. citri mitogenome (OX465514). Reads with homology (a successful BLAST hit) to the mitogenome were used in a Flye (2.8.1-b1676) assembly with 5 iterations. This assembly was then polished with Illumina reads using Perbase (https://github.com/sstadick/perbase, base-depth --max-depth 1000000), and a custom perl script (https://github.com/warrenjessica/Mealybug_mirror_mt-tRNAs/tree/main/Mitogenome_assembly). Bowtie2 v2.5.4 (64) was used to map Illumina reads to the Nanopore assembly.

Mitogenome annotation

tRNA annotation: Mt-tRNA annotation was performed using tRNA search programs and validated with full-length tRNA sequencing. The completed mitogenome assembly was scanned with tRNAscan-SE using the organellar search option (-O), and with MITOS2 under default parameters, using the Metazoa reference database and the invertebrate mitochondrial genetic code. The most frequent start and stop coordinates for each high-abundance YAMAT read were assigned as the tRNA boundaries. These reads were compared to a database of mt-tRNAs from closely related species (Supp.Table 3) using BLASTn (-task blastn, -dust no). Any tRNAs not identified by MITOS2 were assigned to the identity of their closest BLAST match from a relative.

tRNA folding: Each mt-tRNA was manually folded by positioning the predicted anticodon approximately in the center of the tRNA, and any G/C base pairs were predicted to be stabilizing stems.

Protein annotation: Protein-coding gene annotation was performed using a reference amino acid database of mitochondrial proteins from *P. manihoti* (NC_066716). This database was queried against the *P. citri* mitogenome assembly using tBLASTn (-evalue 0.1, -db_gencode 5, -seg no). Regions showing homology to *P. manihoti* genes were searched for the longest ORFs. Homologous regions corresponding to all protein-coding genes were recovered except for ATP8 and ND4L. For these two genes, ORFs were identified within the syntenic regions where they occur in other scale insects, and the resulting ORFs were confirmed by BLASTp against a database of ATP8 and ND4L sequences from related species. When a gene corresponded to multiple ORFs within the P. citri mitogenome, each ORF was annotated as part of the gene (Supp. Table 1).

Full-length tRNA sequencing

Full-length tRNAs where sequenced using YAMAT-seq (16) with a slightly modified protocol described below.

RNA extraction: Total RNA for tRNA sequencing was extracted using 1 mL TRIzol following TRIzol manufacturer's RNA extraction protocol.

Deacylation: For each YAMAT-seq library, 5 µg total RNA was deacylated in 100 mM Tris-pH 9.0 at 37°C for 60 min. This reaction was neutralized by addition of sodium acetate pH 4.8 to a final concentration of 180 mM. Deacylated RNA was ethanol precipitated and resuspended in RNase free H_2O.

Adapter ligation: A 9 µl reaction volume containing 1 µg of deacylated RNA and 1 pmol of each Y-5′ adapter (5 pmols total) and 5 pmols of the Y-3′ adapter was incubated at 90°C for 2 min. A total of 1 µl of an annealing buffer containing 500 mM Tris–HCl (pH 8.0) and 100 mM $MgCl_2$ was added to the reaction mixture and incubated for 15 min at 37°C. Ligation was performed by adding one unit of T4 RNA Ligase 2 enzyme (New England Biolabs) in 10 µl of 1× reaction buffer and incubating the reaction at 37°C for 60 min then incubating at 4°C at 60 min. All adapter and primer sequences can be found in Supp. Table 9.

Reverse transcription: RT of ligated RNA was performed using SuperScript IV (Invitrogen) according to the manufacturer's protocol but with slight modifications. Briefly, 2 µl of 2 µM RT primer, and 2 µl of 10 mM dNTP mix was added to 20 µl of the ligated RNA. The mixture was briefly vortexed, centrifuged and incubated at 70°C for 2 min and the temperature was reduced to 37 °C by 0.1 °C/s. Then, 8 µl of 5× SSIV buffer, 2 µl 100 mM DTT, 2 µl RNaseOUT and 2 µl of SuperScriptIV was added to each reaction. The reaction was incubated for 10 min at 55 °C and then the samples incubated at 35 °C overnight for an overnight RT reaction.

Size selection of the cDNA: To remove free adapters and adapter dimers, a size selection was done on the cDNA products prior to PCR. cDNA was size selected on the BluePippin (Sage

Science), using 3% agarose gel cassettes and marker Q3 following the manufacturer's protocol. The size selection parameters were set to a range of 90-200 bp. Size-selected cDNA was then cleaned using solid phase reversible immobilization beads (1.8X ratio) and resuspended in 10 mM Tris-pH 8.0.

PCR: The resulting cDNA was amplified by polymerase chain reaction (PCR) in a 50 µl reaction containing 20 µl of the size selected cDNA, 25 µl of the NEBNext 2× PCR Master Mix, 2.5 µl of the PCR forward primer, 2.5 µl of the PCR reverse primer. Seven cycles of PCR were performed with an initial 1 min incubation at 98°C and 7 cycles of 30 s at 98°C, 30 s at 60°C and 30 s at 72°C, followed by 5 min at 72°C. PCR products were cleaned using solid phase reversible immobilization beads (1.6X ratio) and resuspended in 10 mM Tris (pH 8.0). Libraries were sequenced on an Illumina NovaSeq X Plus with paired-end, 150-bp reads.

YAMAT-seq read mapping, differential abundance analysis, and tRNA modification indexes

All YAMAT-seq data processing scripts can be found at https://github.com/warrenjessica/Mealybug_mirror_mt-tRNAs/

Reference database for mapping: The nuclear *P. citri* tRNA reference was generated by scanning the Wellcome nuclear assembly (GCA_950023065) with tRNAscan-SE using the general search option (-G). Mt-tRNA references were determined previously (see annotation section above). The endosymbiont tRNA databases were based on previously published assemblies (CP002244 and NC_015735). Combined tRNA database can be found at (Supp. Table 4).

Read mapping: Reads were either mapped globally to the mitogenome using BLAST (blastn -dust no) to measure detection of tRNA reads from all positions on the mitogenome, or reads were mapped to the combined nuclear, mitochondrial, and endosymbiont tRNA database using a previously described pipeline (65).

Differential abundance analysis: Three YAMAT-seq libraries were made from gradient-purified mitochondria, and three YAMAT-seq libraries were made from total insect RNA (three whole insects were homogenized in TRIzol per replicate). Differential abundance analysis was then performed on mapped read counts using EdgeR (66) (Supp. table 6).

tRNA modification index: Generation of a tRNA modification index was done with a pre-existing pipeline (65). A tRNA position was considered modified if >20% of the mapped reads to the reference had a misincorporation at this position.

Aminoacylation assay

To measure tRNA expression and infer aminoacylation states based on retention of CCA tails, an MSR-seq protocol (30) was performed on three biological replicates from three gradient-purified mitochondrial samples, both with and without periodate treatment. Library construction, sequencing, and data analysis were performed as described previously (43), except that a series of lowered PCR cycles was performed (6 and 10 cycles) in addition to the 15 cycles used in the published protocol. The reference tRNA set for mapping included combined *P.citri* database (Supp. Table 4) and a Bacillus subtilis tRNA-Ile that was synthesized and used as an internal "spike-in" control as described previously (43).

Mitoribosome tRNA-seq

Mitochondrial ribosomes were isolated from crudely isolated mitochondria. Each mitoribosome isolation used three pooled, crude mitochondrial isolations, totaling approximately 6 g of mealybugs. Mitochondria were resuspended in 1.5 mL of lysis buffer containing 25 mM HEPES-

KOH, pH 7.4, 150 mM KCl, 50 mM MgOAc, 1.5% β-DDM, 0.15 mg/ml Cardiolipin, 2 mM DTT, 10 mM chloramphenicol, 10 mM cycloheximide, and a Pierce Protease Inhibitor Mini Tablets, EDTA-free (1 tablet/10 ml). Solution was transferred to a 2 mL glass dounce and dounced 20x with the tight pestle avoiding the generation of bubbles. Homogenized mitochondria were placed on a roller for 30 min at 4°C to complete mitochondrial lysis. The homogenate was spun at 25,000g for 20 min at 4°C in a fixed angle rotor to remove insoluble material. Pellet was discarded by carefully decanting the supernatant. Supernatant was then layered on top of a 2.5 mL 1M sucrose cushion (1M sucrose, 20 mM HEPES, 100 mM KCl, 20 mM MgOAc, 0.6% B-DDM, 0.06 mg/ml Cardiolipin, 2 mM DTT). The sample was centrifuged for 230,000g for 90 min at 4 °C. The supernatant was discarded, and the pellet was carefully washed with resuspension (20 mM HEPES-KOH, pH 7.4,100 mM KCl, 10 mM MgOAc, 0.15% β-DDM, 0.015 mg/ml Cardiolipin, 2 mM DTT) buffer to remove residual sucrose. Ribosome pellet was gently resuspended in a fresh 300 µl resuspension buffer by rocking back and forth, using vortex on a very low speed, and gentle pipetting. The resuspended ribosomes were then layered on top of a 10-40% continuous sucrose gradient (in 20 mM HEPES-KOH, pH 7.4, 100 mM KCl, 10 mM MgOAc, 2 mM DTT, created with the BioComp Gradient Master) and spun in a Beckman Ti 40 rotor at 200,000g for 200 min at 4 °C. Gradients were fractionated using a BioComp Piston Gradient Fractionator while measuring the 260 nm absorption to identify ribosome fractions. Fractions containing mitoribosomes were pooled, and RNA was extracted using TRIzol using manufacturer's RNA extraction protocol. YAMAT libraries were then constructed from the resulting RNA.

Identification of ribosomes in sucrose gradient fractions: Total RNA was extracted from the sucrose gradient fractions 5-12 separately and RT-qPCR was used to determine the relative abundance of each ribosome type in the gradient. 100 ng of RNA from each fraction was reverse transcribed (iScript Reverse Transcription Supermix, Bio-rad) using manufacturer's protocol. 1 µl of the cDNA reaction mixture for each fraction was then subjected to qPCR targeting primers for the large ribosomal rRNA from the cytosolic, mitochondrial, and endosymbiont ribosomes (primers can be found in Supp. Table 10B).

PacBio IsoSeq

Isoseq read processing: IsoSeq libraries were created from two biological replicates of total insect RNA and two biological replicates of dissected bacteriome tissue (specialized organ tissue). Libraries were constructed with the SMRTbell prep kit 3.0 (v02.2022) and sequenced on the PacBio Revio instrument. Adapters and poly-A tails were trimmed using cutadapt 5.1 to use the --poly-a option.

IsoSeq read mapping and ORF searches: All trimmed IsoSeq reads were BLASTed (blastn -dust no -evalue 1e-6, query_coverage > 90, percent_identity > 90) to the *P.citri* mitogenome assembly to find high confidence mitochondrial reads. These reads were then searched for all ORFs using the EMBOSS: getorf program (-table 5 -find 1 -minsize 300). All ORFS were then BLASTed to the *P. manihoti* protein coding sequences (tblastn -evalue 1e-6 -seg no) to find homologous ORFs.

Proteomics

Peptides were isolated and sequenced from gradient-purified *P. citri* mitochondria at the Arizona State University Mass Spectrometry Facility. Peptides were injected onto an Ultimate 3000 HPLC (Thermo Fisher Scientific) at 0.300 nL/min and separated on a 50 cm EASY SPRAY C18 column (Thermo Fisher Scientific) before being analyzed in an Orbitrap Fusion Lumos Tribrid Mass Spectrometer (Thermo Fisher Scientific). The mass spectrometer was run in database-dependent acquisition (DDA) mode with both MS1 and MS2 being detected on the Orbitrap. The MS1 full scan resolution was set to 120K, a scan range of 375-1500 m/z, charge states were set to the range of +2 to +7, the AGC target was set to 400K, and maximum injection time was 50ms.

Precursor ions were activated by HCD with 30% collision energy, MS2 resolution was set to 30K, the AGC target was set to 50K, and the maximum injection time was 54ms. Raw data files were analyzed in Proteome Discoverer 3.1 (Thermo Fisher Scientific).

Acknowledgments

We thank Courtney York for the mealybug husbandry. J.M.W. was supported by an HHMI Hanna H. Gray Fellowship, and K.V.S.K.P was supported by a grant from the National Science Foundation (MCB-2322154).

Data availability

All YAMAT- and MSR-seq reads were deposited on Genbank BioProject (Accession PRJNA1356551). All scripts used for analysis can be found at https://github.com/warrenjessica/Mealybug_mirror_mt-tRNAs

References

1. C. Saccone, *et al.*, Mitochondrial DNA in metazoa: degree of freedom in a frozen event. *Gene* **286**, 3–12 (2002).

2. M. A. T. Rubio, *et al.*, Mammalian mitochondria have the innate ability to import tRNAs by a mechanism distinct from protein import. *Proc. Natl. Acad. Sci. U.S.A.* **105**, 9186–9191 (2008).

3. K. Watanabe, Unique features of animal mitochondrial translation systems. The non-universal genetic code, unusual features of the translational apparatus and their relevance to human mitochondrial diseases. *Proc Jpn Acad Ser B Phys Biol Sci* **86**, 11–39 (2010).

4. A. Schneider, Mitochondrial tRNA import and its consequences for mitochondrial translation. *Annu Rev Biochem* **80**, 1033–1053 (2011).

5. T. Salinas-Giegé, R. Giegé, P. Giegé, tRNA biology in mitochondria. *Int J Mol Sci* **16**, 4518–4559 (2015).

6. M. Neiman, D. R. Taylor, The causes of mutation accumulation in mitochondrial genomes. *Proc Biol Sci* **276**, 1201–1209 (2009).

7. M. Lynch, Mutation accumulation in transfer RNAs: molecular evidence for Muller's ratchet in mitochondrial genomes. *Mol Biol Evol* **13**, 209–220 (1996).

8. M. Lynch, Mutation accumulation in nuclear, organelle, and prokaryotic transfer RNA genes. *Molecular Biology and Evolution* **14**, 914–925 (1997).

9. B. Kuhle, J. Chihade, P. Schimmel, Relaxed sequence constraints favor mutational freedom in idiosyncratic metazoan mitochondrial tRNAs. *Nat Commun* **11**, 969 (2020).

10. F. Jühling, J. Pütz, C. Florentz, P. F. Stadler, Armless mitochondrial tRNAs in Enoplea (Nematoda). *RNA Biol* **9**, 1161–1166 (2012).

11. J. Pons, P. Bover, L. Bidegaray-Batista, M. A. Arnedo, Arm-less mitochondrial tRNAs conserved for over 30 millions of years in spiders. *BMC Genomics* **20**, 665 (2019).

12. J. M. Warren, D. B. Sloan, Hopeful monsters: unintended sequencing of famously malformed mite mitochondrial tRNAs reveals widespread expression and processing of sense–antisense pairs. *NAR Genomics and Bioinformatics* **3**, lqaa111 (2021).

13. A. Butenko, J. Lukeš, D. Speijer, J. G. Wideman, Mitochondrial genomes revisited: why do different lineages retain different genes? *BMC Biol* **22**, 15 (2024).

14. P. P. Chan, B. Y. Lin, A. J. Mak, T. M. Lowe, tRNAscan-SE 2.0: improved detection and functional classification of transfer RNA genes. *Nucleic Acids Research* **49**, 9077–9096 (2021).

15. M. Bernt, *et al.*, MITOS: Improved de novo metazoan mitochondrial genome annotation. *Molecular Phylogenetics and Evolution* **69**, 313–319 (2013).

16. M. Shigematsu, *et al.*, YAMAT-seq: an efficient method for high-throughput sequencing of mature transfer RNAs. *Nucleic Acids Res* **45**, e70 (2017).

17. J. M. Warren, *et al.*, Combining tRNA sequencing methods to characterize plant tRNA expression and post-transcriptional modification. *RNA Biol* **18**, 64–78 (2021).

18. K. Watanabe, S.-I. Yokobori, tRNA Modification and Genetic Code Variations in Animal Mitochondria. *J Nucleic Acids* **2011**, 623095 (2011).

19. J. M. Warren, *et al.*, Rapid Shifts in Mitochondrial tRNA Import in a Plant Lineage with Extensive Mitochondrial tRNA Gene Loss. *Mol Biol Evol* **38**, 5735–5751 (2021).

20. R. Lorenz, *et al.*, ViennaRNA Package 2.0. *Algorithms Mol Biol* **6**, 26 (2011).

21. T. Suzuki, The expanding world of tRNA modifications and their disease relevance. *Nat Rev Mol Cell Biol* **22**, 375–392 (2021).

22. S. K. Schultz, *et al.*, Modifications in the T arm of tRNA globally determine tRNA maturation, function, and cellular fitness. *Proc. Natl. Acad. Sci. U.S.A.* **121**, e2401154121 (2024).

23. W. C. Clark, M. E. Evans, D. Dominissini, G. Zheng, T. Pan, tRNA base methylation identification and quantification via high-throughput sequencing. *RNA* **22**, 1771–1784 (2016).

24. V. Potapov, *et al.*, Base modifications affecting RNA polymerase and reverse transcriptase fidelity. *Nucleic Acids Res* **46**, 5753–5763 (2018).

25. R. Hauenschild, *et al.*, The reverse transcription signature of N-1-methyladenosine in RNA-Seq is sequence dependent. *Nucleic Acids Res* **43**, 9950–9964 (2015).

26. K. Katoh, J. Rozewicki, K. D. Yamada, MAFFT online service: multiple sequence alignment, interactive sequence choice and visualization. *Brief Bioinform* **20**, 1160–1166 (2019).

27. T. Suzuki, *et al.*, Complete chemical structures of human mitochondrial tRNAs. *Nat Commun* **11**, 4269 (2020).

28. Y. Nakano, *et al.*, Genome-wide profiling of tRNA modifications by Induro-tRNAseq reveals coordinated changes. *Nat Commun* **16**, 1047 (2025).

29. D. V. Lavrov, W. M. Brown, J. L. Boore, A novel type of RNA editing occurs in the mitochondrial tRNAs of the centipede Lithobius forficatus. *Proc Natl Acad Sci U S A* **97**, 13738–13742 (2000).

30. C. P. Watkins, W. Zhang, A. C. Wylder, C. D. Katanski, T. Pan, A multiplex platform for small RNA sequencing elucidates multifaceted tRNA stress response and translational regulation. *Nat Commun* **13**, 2491 (2022).

31. K. Davidsen, L. B. Sullivan, A robust method for measuring aminoacylation through tRNA-Seq. *bioRxiv* 2023.07.31.551363 (2024). https://doi.org/10.1101/2023.07.31.551363.

32. I. Kozarewa, *et al.*, Amplification-free Illumina sequencing-library preparation facilitates improved mapping and assembly of (G+C)-biased genomes. *Nat Methods* **6**, 291–295 (2009).

33. S. Aibara, J. Andréll, V. Singh, A. Amunts, Rapid Isolation of the Mitoribosome from HEK Cells. *J Vis Exp* 57877 (2018). https://doi.org/10.3791/57877.

34. A. Brown, *et al.*, Structure of the large ribosomal subunit from human mitochondria. *Science* **346**, 718–722 (2014).

35. J. P. Adelman, C. T. Bond, J. Douglass, E. Herbert, Two Mammalian Genes Transcribed from Opposite Strands of the Same DNA Locus. *Science* **235**, 1514–1517 (1987).

36. Y. A. Khan, *et al.*, Evidence for a novel overlapping coding sequence in POLG initiated at a CUG start codon. (2020). https://doi.org/10.17863/CAM.56759.

37. V. Pelechano, L. M. Steinmetz, Gene regulation by antisense transcription. *Nat Rev Genet* **14**, 880–893 (2013).

38. J. Ferrer, N. Dimitrova, Transcription regulation by long non-coding RNAs: mechanisms and disease relevance. *Nat Rev Mol Cell Biol* **25**, 396–415 (2024).

39. A. R. D'Souza, M. Minczuk, Mitochondrial transcription and translation: overview. *Essays Biochem* **62**, 309–320 (2018).

40. Z. Pietras, *et al.*, Controlling the mitochondrial antisense - role of the SUV3-PNPase complex and its co-factor GRSF1 in mitochondrial RNA surveillance. *Mol Cell Oncol* **5**, e1516452 (2018).

41. G. Santonoceto, A. Jurkiewicz, R. J. Szczesny, RNA degradation in human mitochondria: the journey is not finished. *Hum Mol Genet* **33**, R26–R33 (2024).

42. K. Pawar, *et al.*, Exploration of CCA-added RNAs revealed the expression of mitochondrial non-coding RNAs regulated by CCA-adding enzyme. *RNA Biol* **16**, 1817–1825 (2019).

43. L. F. Ceriotti, J. M. Warren, M. V. Sanchez-Puerta, D. B. Sloan, The landscape of Arabidopsis tRNA aminoacylation. *Plant J* **120**, 2784–2802 (2024).

44. I. Ozerova, *et al.*, Aberrant Mitochondrial tRNA Genes Appear Frequently in Animal Evolution. *Genome Biol Evol* **16**, evae232 (2024).

45. H. Schürer, S. Schiffer, A. Marchfelder, M. Mörl, This Is the End: Processing, Editing and Repair at the tRNA 3-Terminus. *Biological Chemistry* **382** (2001).

46. K. Tomita, T. Ueda, K. Watanabe, RNA Editing in the Acceptor Stem of Squid Mitochondrial tRNATyr. *Nucleic Acids Research* **24**, 4987–4991 (1996).

47. A. Reichert, U. Rothbauer, M. Mörl, Processing and Editing of Overlapping tRNAs in Human Mitochondria. *Journal of Biological Chemistry* **273**, 31977–31984 (1998).

48. V. Doublet, *et al.*, Large gene overlaps and tRNA processing in the compact mitochondrial genome of the crustacean Armadillidium vulgare. *RNA Biol* **12**, 1159–1168 (2015).

49. V. Doublet, C. Souty-Grosset, D. Bouchon, R. Cordaux, I. Marcadé, A thirty million year-old inherited heteroplasmy. *PLoS One* **3**, e2938 (2008).

50. Z. Chrzanowska-Lightowlers, J. Rorbach, M. Minczuk, Human mitochondrial ribosomes can switch structural tRNAs - but when and why? *RNA Biol* **14**, 1668–1671 (2017).

51. S. E. Masta, The Complete Mitochondrial Genome Sequence of the Spider Habronattus oregonensis Reveals Rearranged and Extremely Truncated tRNAs. *Molecular Biology and Evolution* **21**, 893–902 (2004).

52. P. B. Klimov, B. M. Oconnor, Improved tRNA prediction in the American house dust mite reveals widespread occurrence of extremely short minimal tRNAs in acariform mites. *BMC Genomics* **10**, 598 (2009).

53. X.-F. Xue, W. Deng, S.-X. Qu, X.-Y. Hong, R. Shao, The mitochondrial genomes of sarcoptiform mites: are any transfer RNA genes really lost? *BMC Genomics* **19**, 466 (2018).

54. D. R. Wolstenholme, J. L. Macfarlane, R. Okimoto, D. O. Clary, J. A. Wahleithner, Bizarre tRNAs inferred from DNA sequences of mitochondrial genomes of nematode worms. *Proc. Natl. Acad. Sci. U.S.A.* **84**, 1324–1328 (1987).

55. R. Okimoto, D. R. Wolstenholme, A set of tRNAs that lack either the T psi C arm or the dihydrouridine arm: towards a minimal tRNA adaptor. *The EMBO Journal* **9**, 3405–3411 (1990).

56. H. Seligmann, Undetected antisense tRNAs in mitochondrial genomes? *Biol Direct* **5**, 39 (2010).

57. A. S. Rodin, E. Szathmáry, S. N. Rodin, One ancestor for two codes viewed from the perspective of two complementary modes of tRNA aminoacylation. *Biol Direct* **4**, 4 (2009).

58. S. N. Rodin, S. Ohno, Two types of aminoacyl-tRNA synthetases could be originally encoded by complementary strands of the same nucleic acid. *Orig Life Evol Biosph* **25**, 565–589 (1995).

59. M. Lynch, *The origins of genome architecture* (Sinauer Associates, 2007).

60. D. M. Rand, Mitigating Mutational Meltdown in Mammalian Mitochondria. *PLoS Biol* **6**, e35 (2008).

61. C.-H. Kuo, N. A. Moran, H. Ochman, The consequences of genetic drift for bacterial genome complexity. *Genome Res* **19**, 1450–1454 (2009).

62. K. Tamura, Origins and Early Evolution of the tRNA Molecule. *Life (Basel)* **5**, 1687–1699 (2015).

63. R. Root-Bernstein, Y. Kim, A. Sanjay, Z. F. Burton, tRNA evolution from the proto-tRNA minihelix world. *Transcription* **7**, 153–163 (2016).

64. B. Langmead, S. L. Salzberg, Fast gapped-read alignment with Bowtie 2. *Nat Methods* **9**, 357–359 (2012).

65. J. M. Warren, *et al.*, Combining tRNA sequencing methods to characterize plant tRNA expression and post-transcriptional modification. *RNA Biol* **18**, 64–78 (2021).

66. Y. Chen, L. Chen, A. T. L. Lun, P. L. Baldoni, G. K. Smyth, edgeR v4: powerful differential analysis of sequencing data with expanded functionality and improved support for small counts and larger datasets. *Nucleic Acids Res* **53**, gkaf018 (2025).

67. K. Darty, A. Denise, Y. Ponty, VARNA: Interactive drawing and editing of the RNA secondary structure. *Bioinformatics* **25**, 1974–1975 (2009).

Figures and Tables

A. Abundance of tRNA-seq reads mapped at each position on the mitogenome

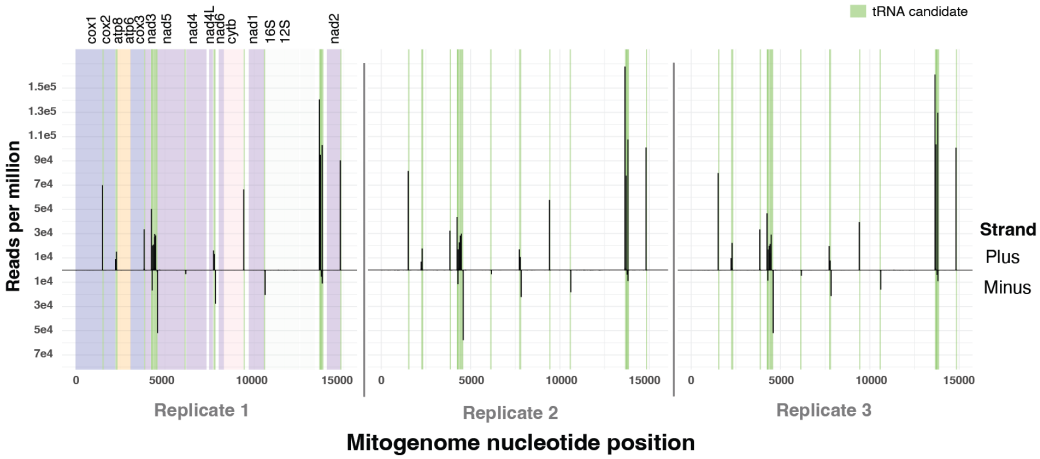

B. Mitogenome organization

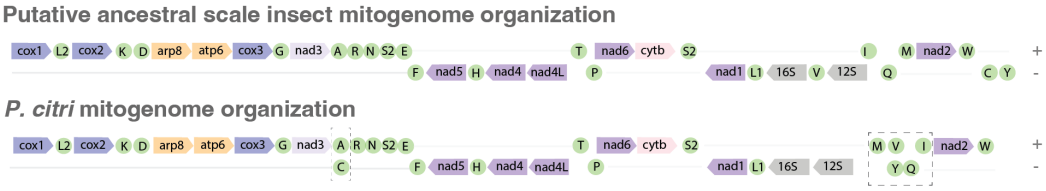

C. Coverage level and coding strands of annotated mt-tRNAs

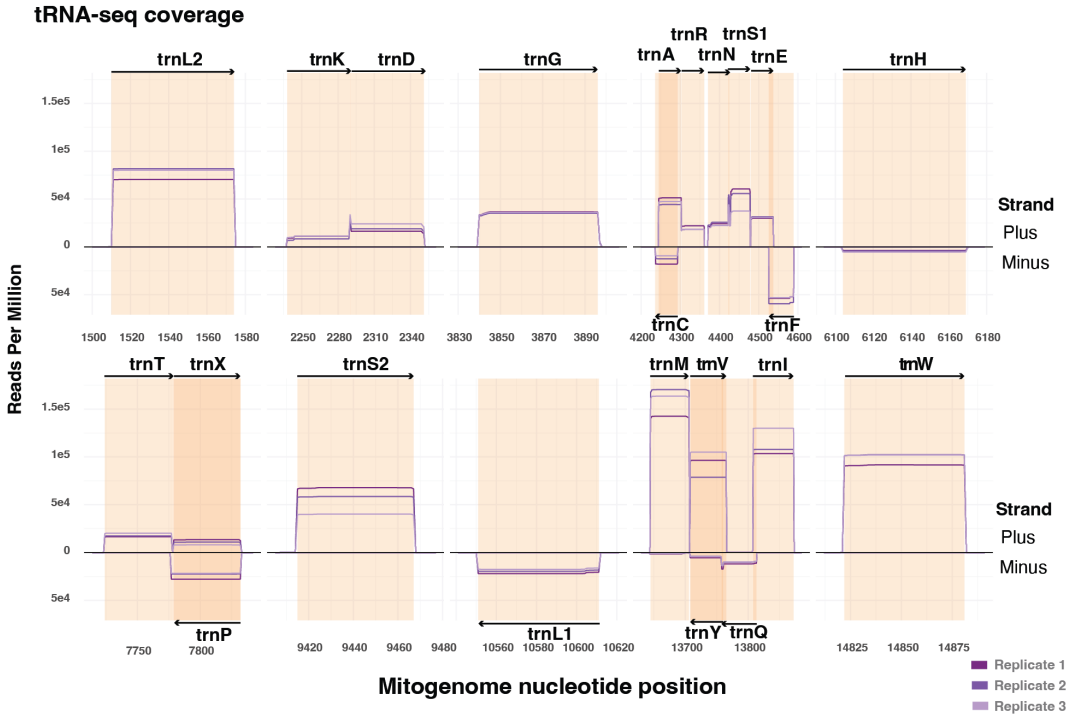

Figure 1. Abundance of CCA-tailed reads mapped to the *P. citri* mitogenome. A. YAMAT-seq read abundances globally mapped across the mitochondrial genome. YAMAT-seq will only capture RNAs with a CCA-overhang and will therefore almost exclusively sequence mature tRNA molecules. Three independent YAMAT-seq libraries were generated from purified mitochondrial fractions. The first replicate plot shows the final protein coding annotations as colored bounds (see protein annotation section for details), and candidate tRNAs are colored in green. Reads aligning to the forward strand are plotted above the x-axis (positive y-values), whereas reads aligning to the reverse strand are plotted below the x-axis (negative y-values). Bars are drawn with a width of 50 bp to visualize local read density, and the average mapped read length is 58 bp. B. Mitogenome organization of the ancestral scale insect and the final annotation of the *P. citri* mitogenome. Mt-tRNA rearrangements are indicated with dashed boxes. C. Detailed read abundance for each of the annotated mt-tRNAs. Darker orange regions indicate where two tRNAs share nucleotides (overlap).

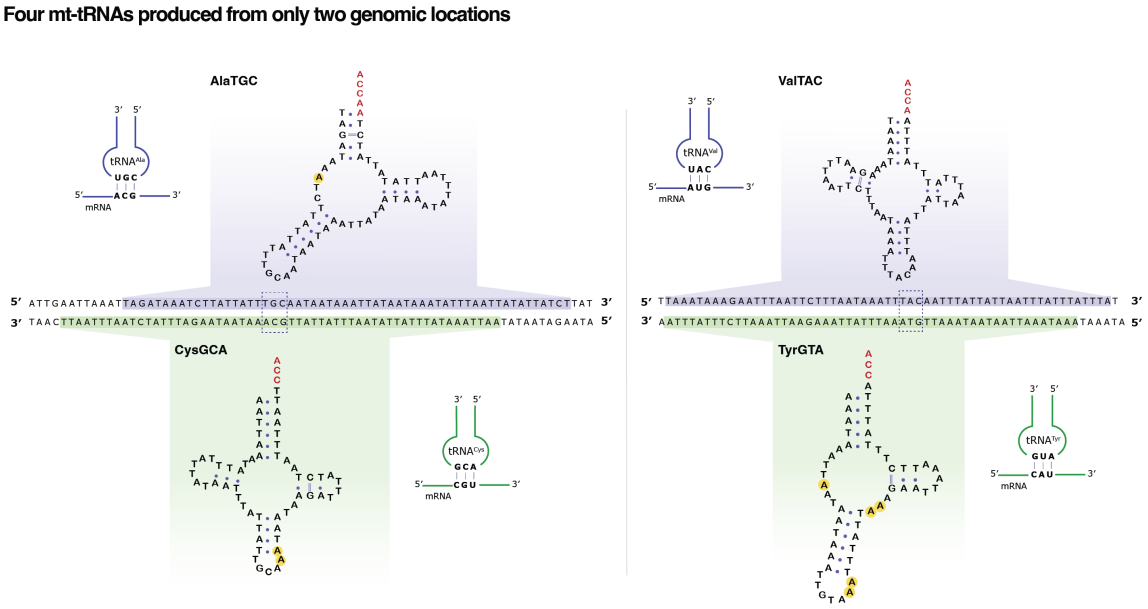

Figure 2. Two loci in the mitogenome produce four tRNAs with different anticodons. The genomic sequence and transcribed strands for each of the mirror mt-tRNAs, Cys/Ala and Tyr/Val. Structures were manually folded to maintain stem and loop features and presented above or below the genomic locus in the mitogenome. Post-transcriptionally added nucleotides are indicated in red. Nucleotides with a yellow circle have evidence of a base modification that interferes with reserve transcription. The genomic coordinates of the anticodon nucleotides (indicated with a dashed box) are the same for each pair of bidirectional tRNAs but are reverse complements of each other and therefore decode for different amino acids. Folded structure diagrams were created using VARNA ver. 3.9 (67).

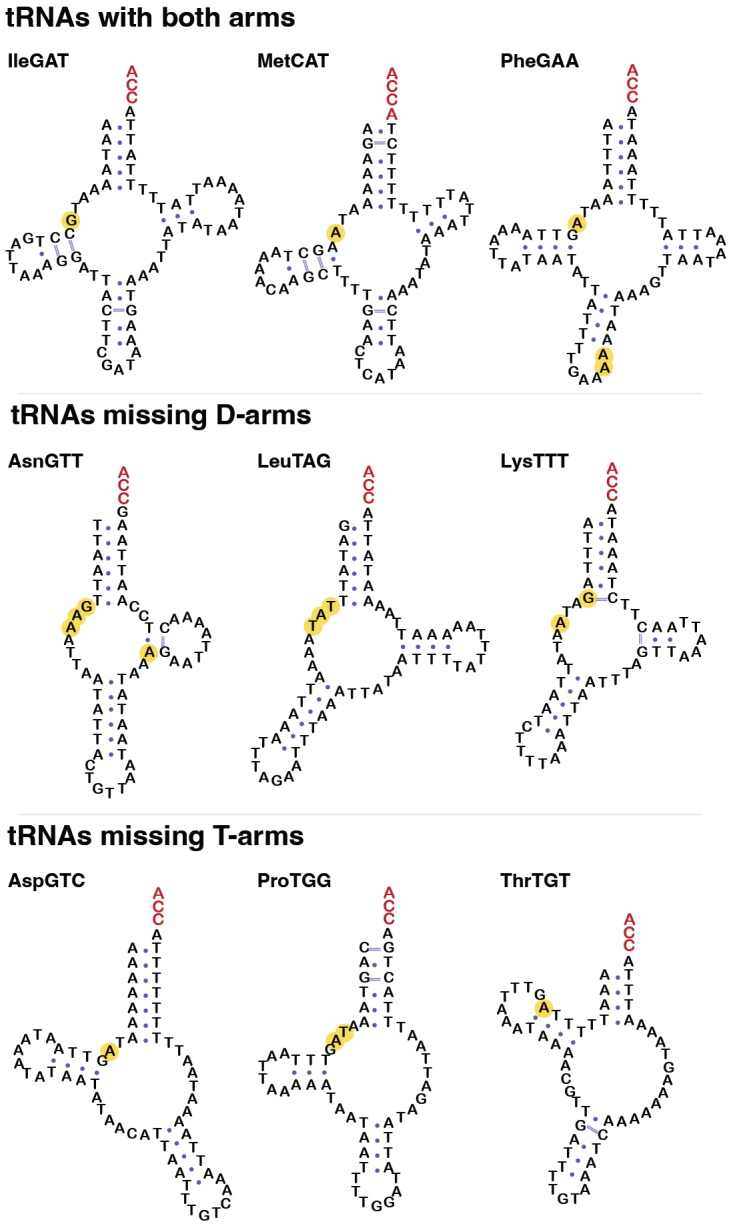

Figure 3. Predicted folding of nine representative mt-tRNAs. Post transcriptionally added nucleotides are indicated in red. Nucleotides with a yellow circle have evidence of a base modification. RNA folding was done manually to maintain stem structures and visualized using VARNA ver. 3.9 (67).

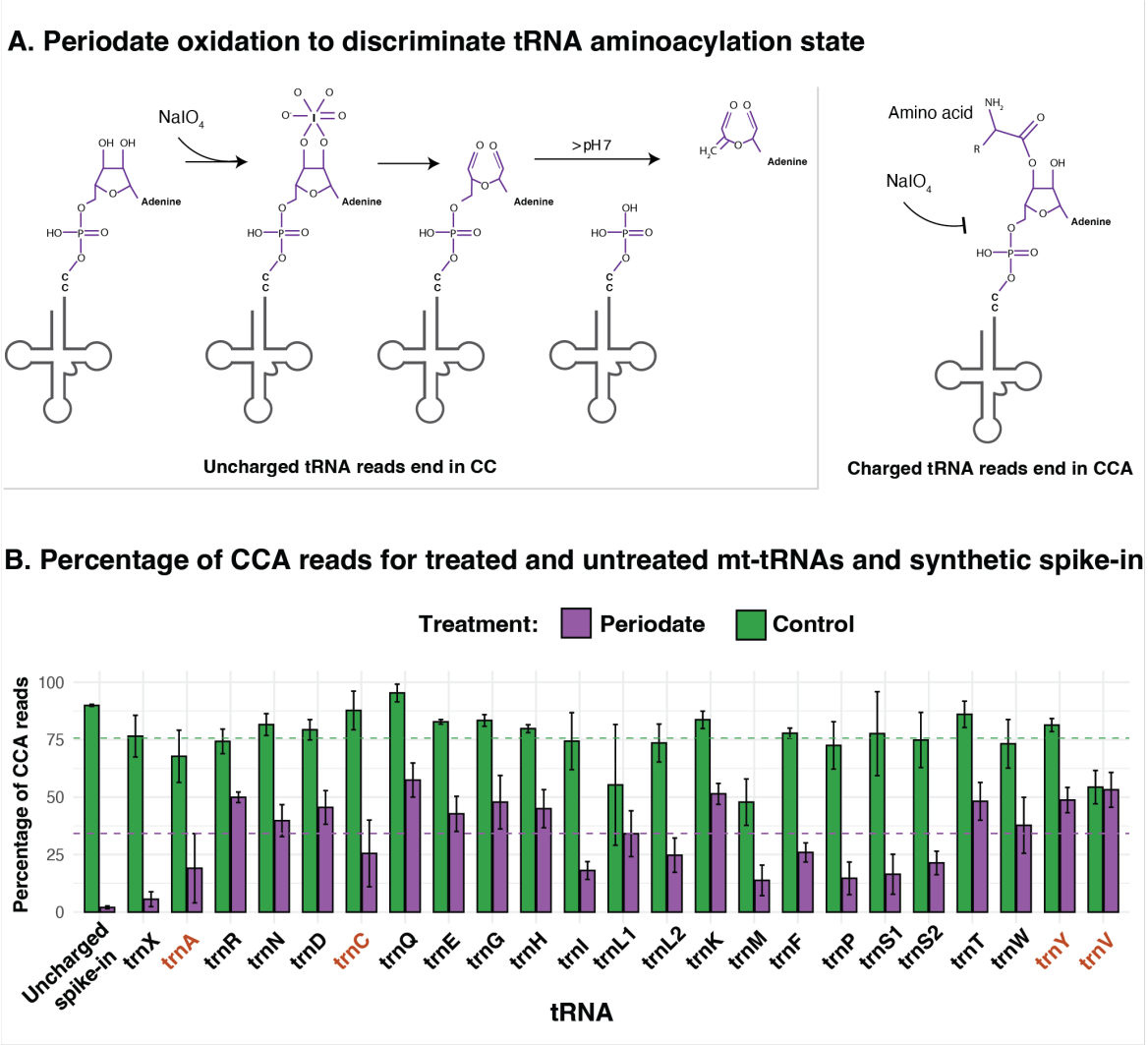

Figure 4. Using periodate oxidation to determine the proportion of charged mt-tRNAs in *P. citri* mitochondria. A. Graphic summary illustrating the use of the Whitfeld reaction followed by 3′ adenosine cleavage to discriminate between deacylated and acylated tRNAs. For uncharged tRNAs the 3′ adenosine is oxidized by periodate and then cleaved off by borax-induced β-elimination. Cleavage of the terminal adenosine means that resulting tRNA-seq reads from uncharged tRNAs end in CC. For charged tRNAs, the 3′ adenosine protected from periodate oxidation and reads will end in CCA. B. Percentage of reads with a complete CCA tail (CCA/(CC+CCA reads) for each mt-tRNA reference and an uncharged, synthetic tRNA. Three total RNA samples from gradient-purified *P. citri* mitochondria were split into periodate and untreated subsamples. Bars represent the average percentage of CCA reads across the three replicates. Error bars indicate ± 1 SD across replicate libraries. Dotted green line is the mean percentage (75.7%) of CCA reads in untreated (control) libraries. Dotted purple line is the mean percentage (34.2%) in periodate treated libraries. Mt-tRNAs in red are the mirror pairs.

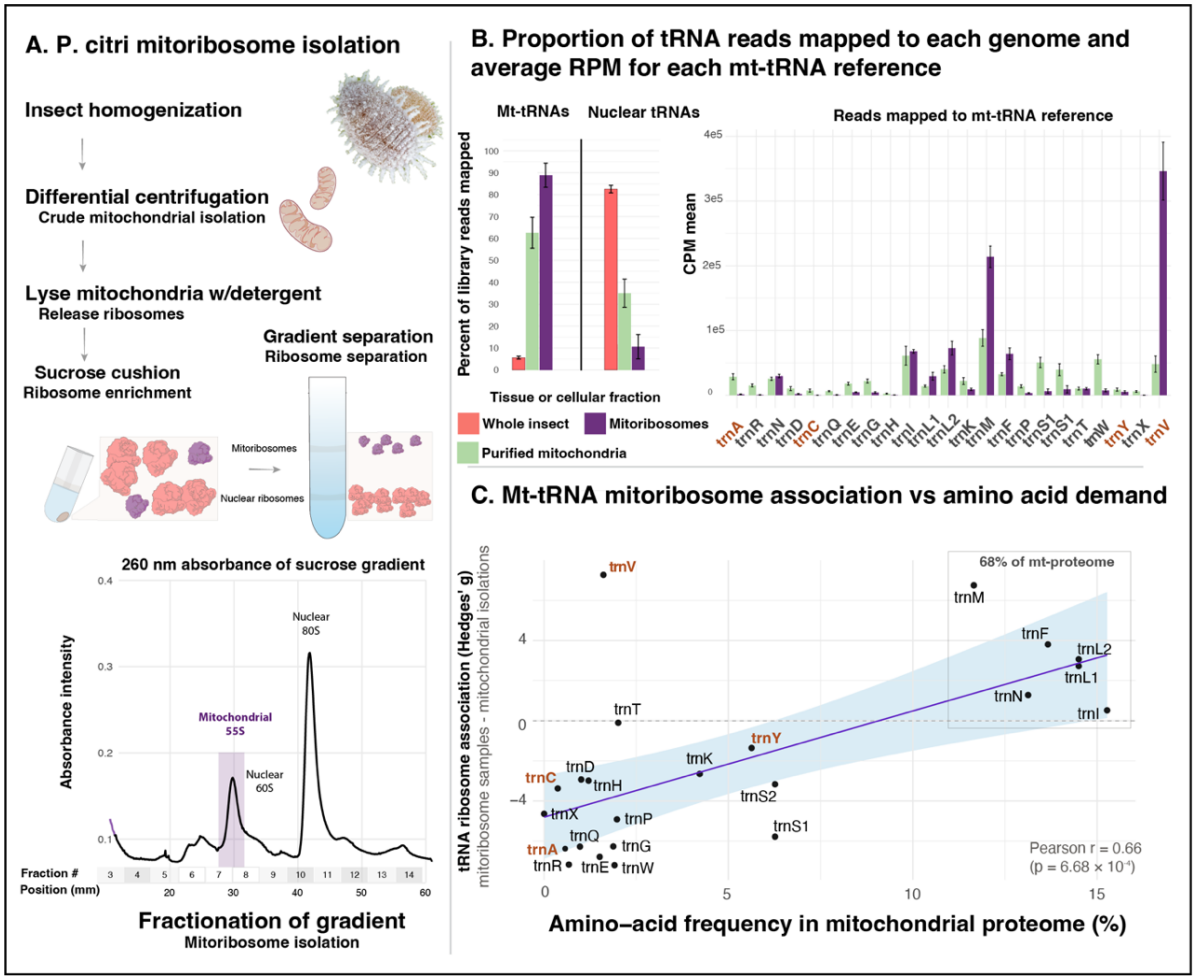

Figure 5. Mitoribosome tRNA sequencing to assess mt-tRNA occupancy. A. Whole mealybugs at multiple life stages were homogenized and subjected to differential centrifugation to enrich for mitochondria. The mitochondrial fraction was lysed with detergents to release mitoribosomes, which were then separated by a sucrose cushion and continuous sucrose gradient to isolate mitoribosomes. The bottom panel shows a representative 260 nm absorbance trace from a sucrose gradient, with the mitochondrial monosomes (intact ribosomes) highlighted in a red box; nuclear large subunit (60S) and monosome (80s) peaks are labeled in text. Total RNA was extracted from the mitoribosome-containing fractions (fractions 6–8) and used to construct mitoribosome tRNA-seq libraries. **B.** Left plot: mean percentage of tRNA-seq reads mapping to the nuclear and mitochondrial genomes from whole-insect, gradient-purified mitochondrial and mitoribosome libraries. Right plot: normalized counts per million (CPM) reads mapping to each mt-tRNA reference from purified mitochondrial and mitoribosome libraries. Error bars indicate ± 1 SD across replicate libraries. Mirror tRNAs are indicated with red text. **C**. Each mt-tRNA's ribosome association versus the frequency of its cognate amino acid in the mitochondrial proteome. Ribosome association was calculated as Hedges' g (mean-difference statistic) for each tRNA, comparing abundance (normalized CPM reads) in mitoribosome libraries versus total mitochondrial libraries. Positive g values indicate higher relative abundance of a tRNA in the ribosome-associated fraction; negative values indicate enrichment in the total mitochondrial libraries. The x-axis shows the frequency of the corresponding amino acid in the mitochondrial proteome. Association strength was evaluated by simple linear regression (g ~ amino-acid frequency). Each point represents a single mt-tRNA; the solid line shows the fitted

regression with its 95% confidence interval (light-green shading). The two pairs of tRNAs with bidirectional expression are highlighted in orange. The boxed region indicates that 68% of the amino acids in the coding sequences are composed of only five amino acids. Amino acid frequencies were determined using homology searches and full-length mRNA sequencing (see protein-coding section below). Mealybug photo in A by Alexander Wild.

Supporting Information for

Supporting Information Text

Supporting File 1. Genbank annotation file for the *P. citri* mitogenome. See Supp.File1.update.txt for annotation file. This file is currently under review by NCBI staff to be deposited on the Genbank server.

Supplementary Figures

A. Full length mRNA sequencing (Iso-seq) of the *P.citri* mitogenome

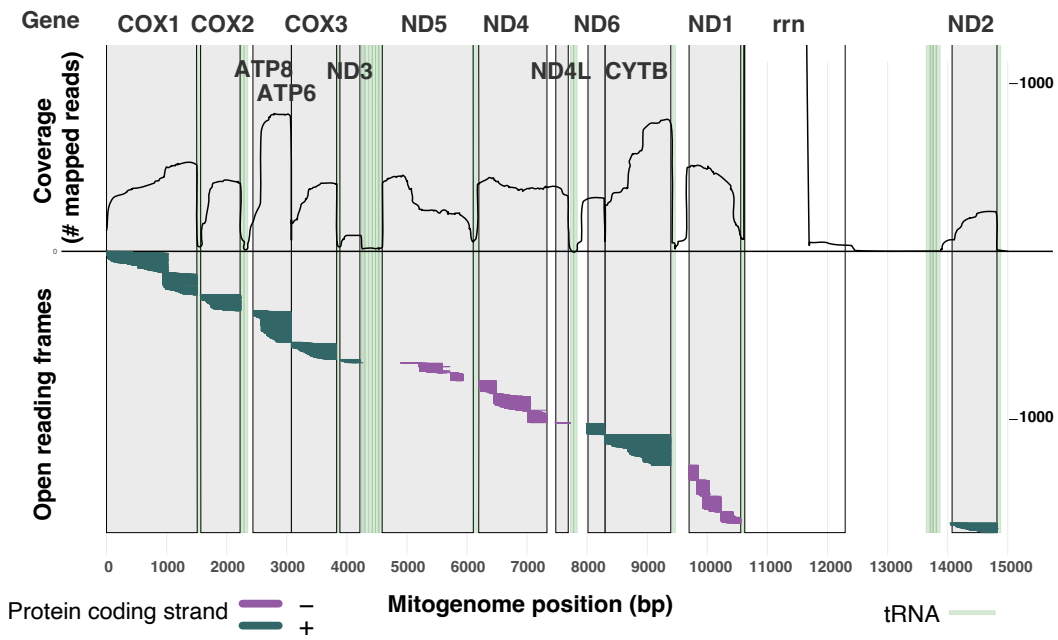

B. COX1 open reading frames

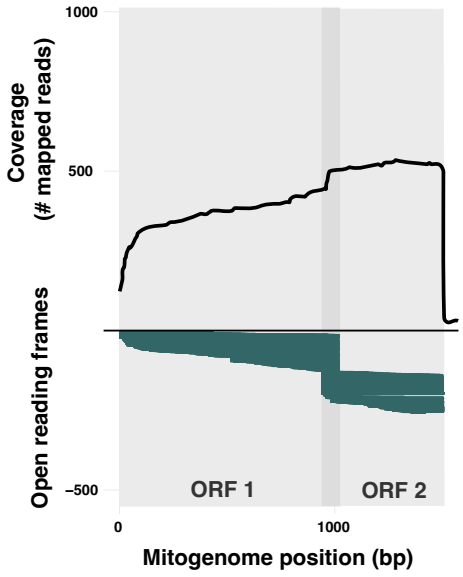

C. Iso-seq length of COX1 mapped reads

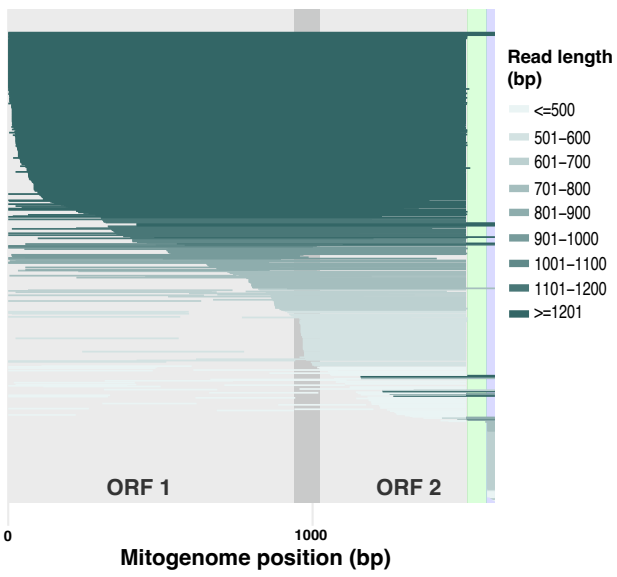

Supplementary Figure 1| IsoSeq coverage and the resulting ORFs for *P. citri* mitochondrial protein-coding genes. A. Top row shows the coverage (number of reads) of IsoSeq reads mapped to the mitogenome with the gene name above. The bottom row shows all the predicted ORFs found in the mapped IsoSeq reads that have homology to *P. manihoti* (blastp, disabled low-complexity filtering, e-value < 1e-6). The coding strand of the ORFs are indicated by color, with genes on the positive strand in green, those on the reverse stand in purple. Genomic locations of mt-tRNA genes are shown in light green shading. COX1, ND1, ND4, and ND5 do not

exist as a single, continuous ORFs, which can be seen from no single ORF spanning the entire region of those genes. B. Detail of the expression level and resulting ORFs of the COX1 gene. The region mapping to the COX1 has two ORFs, with a small amount of overlap (shown in a dark gray stripe). C. IsoSeq reads that map to COX1 region shorted and colored by length. The majority of the IsoSeq reads are greater than 1201 bp and contain both ORFs. Overlap region between the two ORFs is highlighted in a dark gray stripe. Mt-tRNA-Leu(TAA) gene shown in light green stripe immediately to the right of the second COX1 ORF.

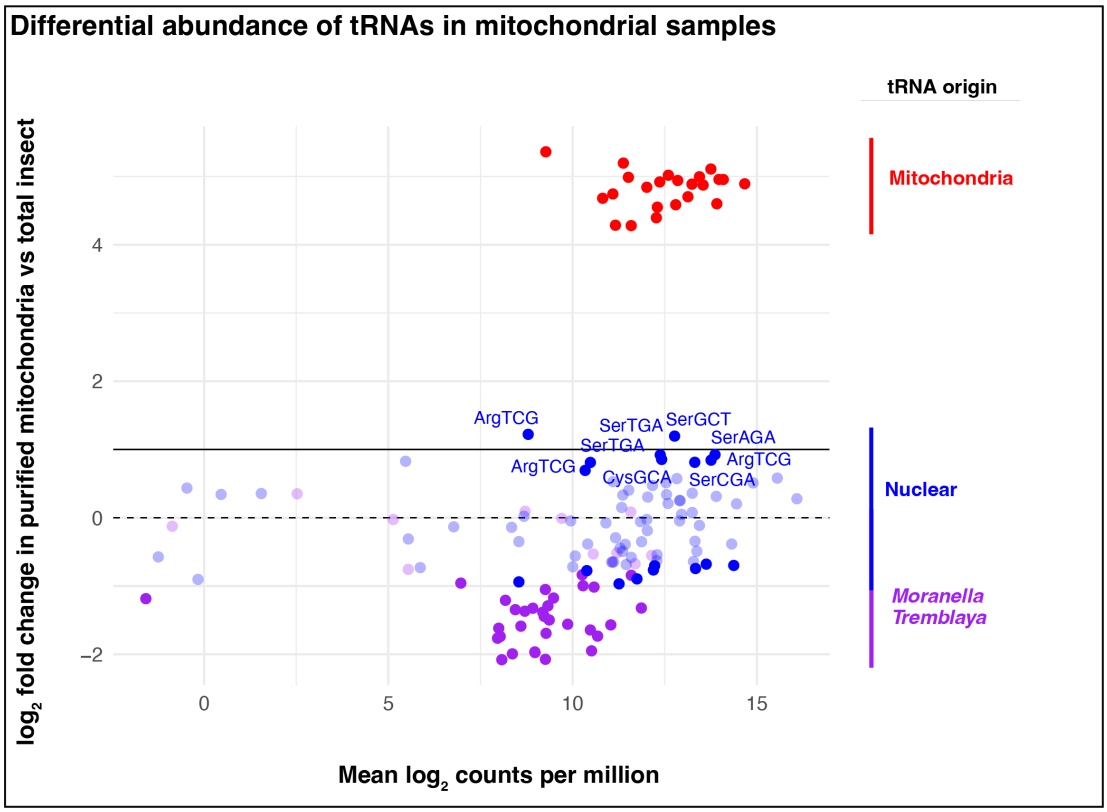

Supplementary Figure 2| Differential abundance of all *P. citri* tRNAs in gradient-purified mitochondria compared to total insect samples. Each point represents a unique tRNA reference and is colored by the encoding genome (mitochondrial tRNAs in red, nuclear tRNAs in blue, and both nutritional endosymbionts tRNAs in purple). Darker dots are tRNAs with an FDR value > 0.05. Dashed line is at 0 (lack of enrichment or depletion), and the thick line is at $\log_2$ fold enrichment of 1 (2x). Nuclear tRNAs with a positive enrichment and an FDR significance > 0.05 are also indicated with the amino acid and anticodon.

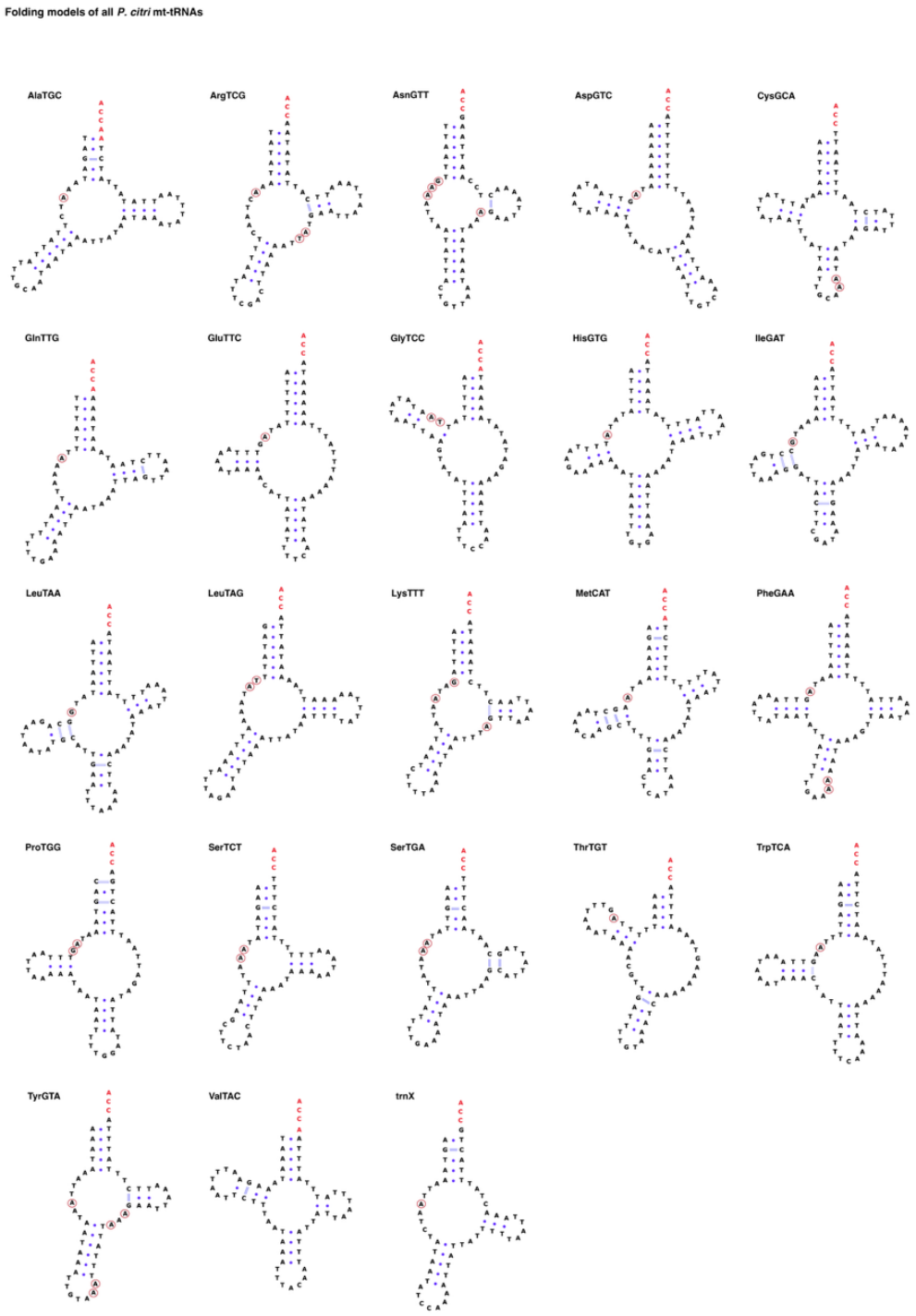

Supplementary Figure 3| Predicted structure diagrams of all *P. citri* mt-tRNA. Mt-tRNAs were manually folded to center anticodon and prioritize stem and loop structure. Red circles indicate a base modification that inhibits reverse transcription (the base is misread in >20% of the reads). Post-transcriptionally added nucleotides are indicated with red font. Folded structure diagrams were created using VARNA ver. 3.9 (67).

Supplementary Figure 4| Modification indexes for all mt-tRNAs. Modification indexes for mt-RNAs in the three mitochondrial isolation YAMAT libraries. A tRNA position was considered modified if >20% of the mapped reads to the reference had a misincorporation at this position. Some tRNAs had slightly overlapping sequences in the mitogenome and the processing of the upstream or downstream tRNA resulted in a truncated sequence that also produced an overhang captured by YAMAT-seq. These sequences produced a variable end (e.g., SerTCT) but were not considered as candidates for base modifications at these positions in this figure or in Supp. Fig. 3.

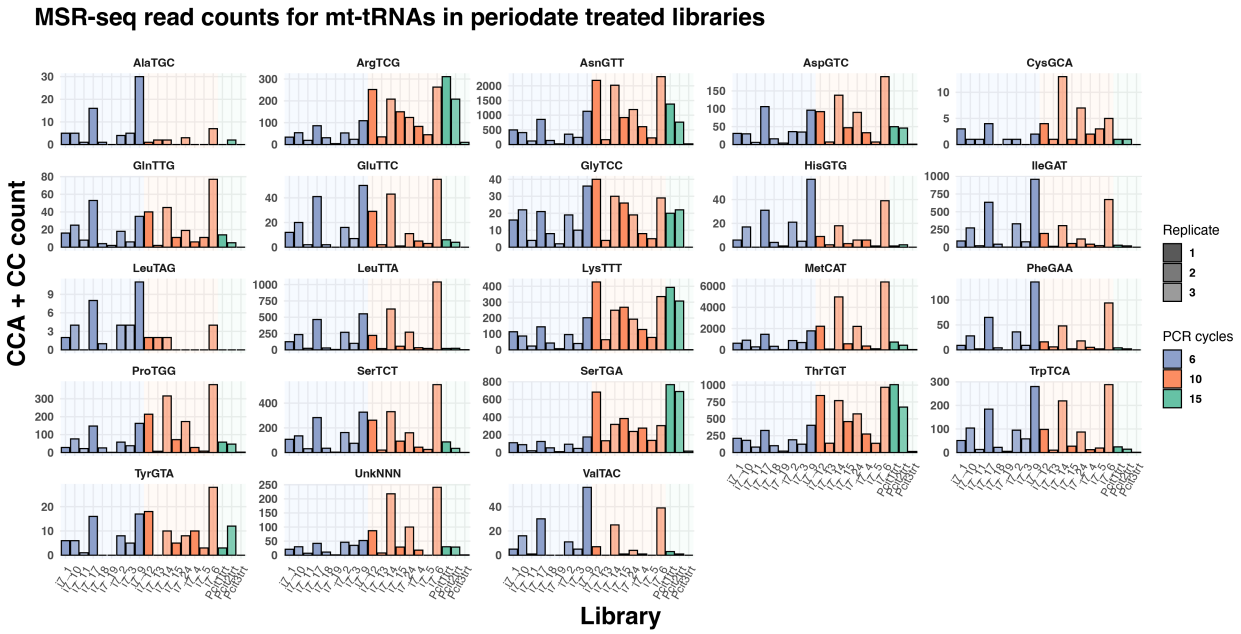

Supplementary Figure 5| Detection of CCA- and CC-ending reads for each mt-tRNA in MSR-seq libraries. Each bar is a separate MSR-seq library specified with its unique barcode identifier. Each library was generated from a separate biological replicate, indicated in shading density. The PCR cycle number used in library amplification is indicated by a different color.

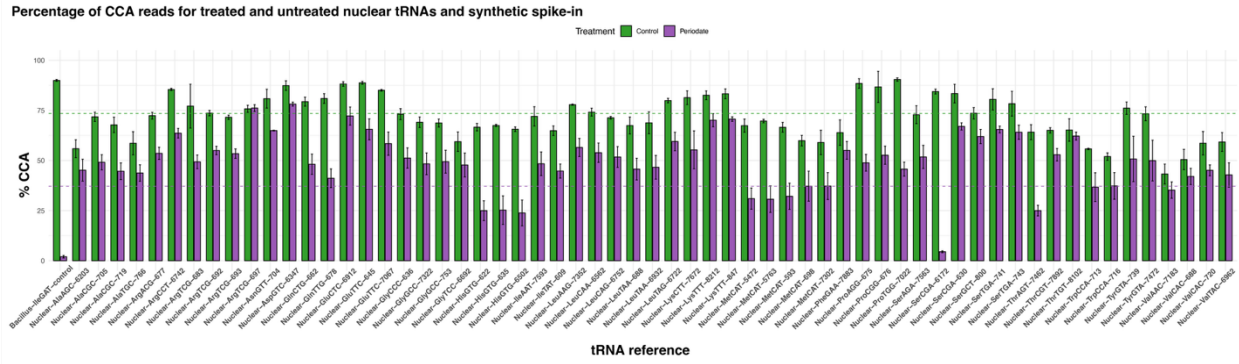

Supplementary Figure 6| Percentage of reads ending in CCA or CC for nuclear *P. citri* tRNAs. Only nuclear tRNAs with at least 1,000 reads combined in both the periodate treated and untreated libraries are shown. Total MSR-seq read counts for all references can be found in Supp. Table 8.

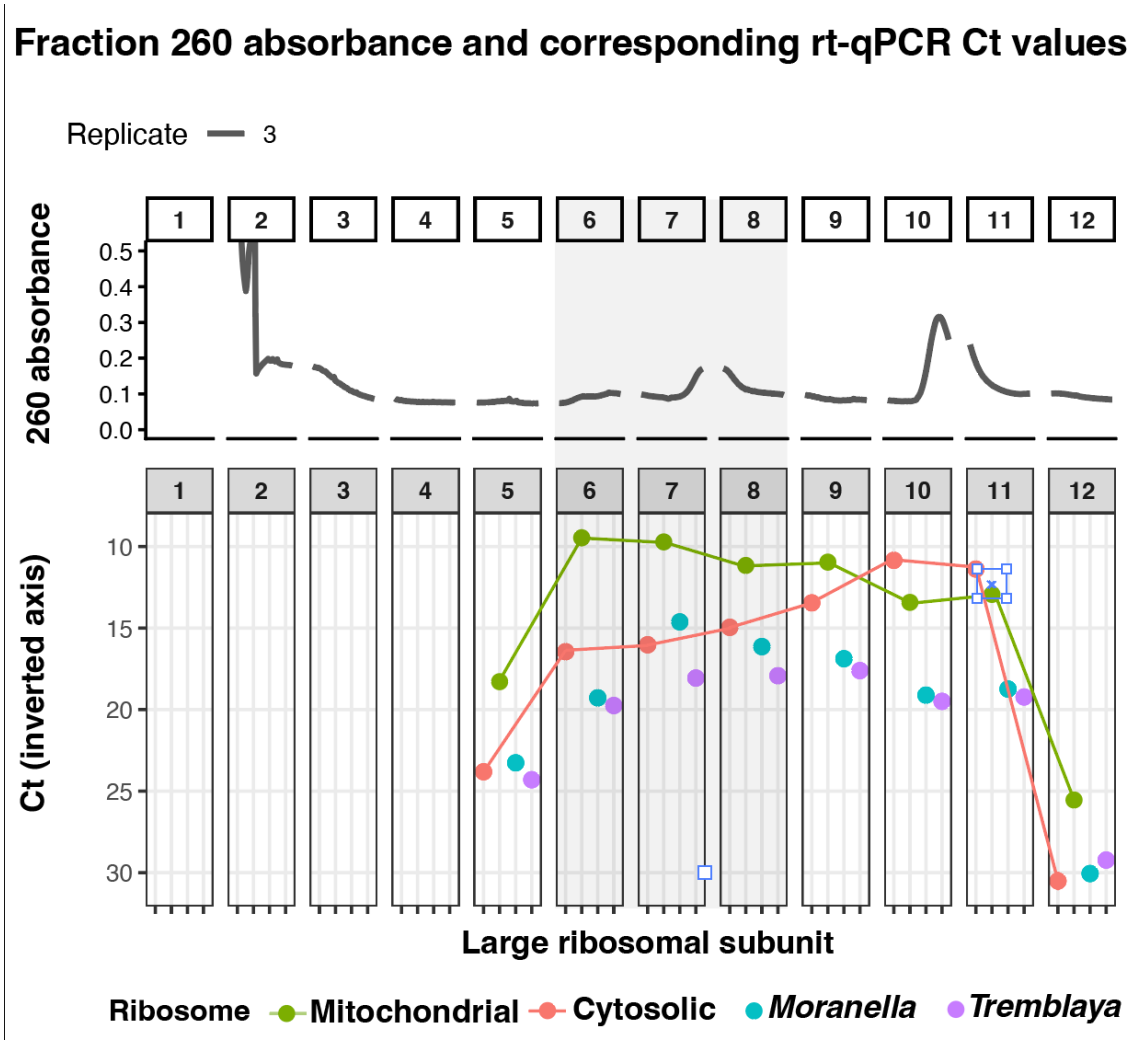

Supplementary Figure 7| rRNA distribution across sucrose gradient fractions. 260-nm absorbance profile (top) and corresponding RT-qPCR cycle threshold (Ct) values for large-subunit rRNA markers across sucrose gradient fractions. Ct values (bottom; inverted axis) are shown for mitochondrial, cytosolic, and the two endosymbiont ribosomes (*Moranella* and *Tremblaya*). All samples were normalized to 5 ng of cDNA for qPCR. Lower Ct values indicate higher rRNA abundance in a fraction. Points represent the mean of three qPCR replicates. The 260-nm absorbance trace is shown for experimental replicate 3.

Supplementary Tables

Table S1. Protein coding ORFs in the *P. citri* mitogenome

Supplementary table 1l Protein coding ORFs in the P. citri mitogenome

Gene.ORF	Start	Stop	Strand	Predicted frameshift position	Amino acid sequence ORF
cox1.1	1	1023	+	+1 frameshift at position 960	MYSTNHKNISLMYLLFGFWSGLMGLSMSFIIRIELMNLNNNFNNNMIYYMMITIHAFIMIFFMTMPIIIGSLSNWLLPLMLMSSDLIFPRLNNFSFWLLIPSLILMMMNMMLSNNINT
cox1.2	939	1511	+	+1 frameshift at position 960	MNNNFKWKKILNSSINFWSIGFIIMFTLGGLTGIILSNSIIDINLHDTYFVVAHFHYVLSMGVIFSIFSSFIFWSPLLFNVSLNNNWLKINFFNLFLSINLTFFPQHFLGMNGMPRRYIMYS
cox2	1572	2237	+	Single ORF	MIISWFMIYFQNNFSFNMIMLNKLNNYIMIIMMMIMMIMFIIIYMNLFIYLNKFNNKMLIENNLIEIIWTIIPLIIILFIAMPSIKVLYLNNEMKTNILSIKIISNQWFWYYEYLNFNNKFNSYMM
atp8	2351	2461	+	Single ORF	MIQFMPNMWILLMIFNMMMFLMNFFINYFSSNKFKF
atp6	2467	3078	+	Single ORF	MFTIFDPYIMNYPMNYFLTIMFMIYLFKKNFWLNNLNMINLFNNNFNNNINQNNPIMNKTIFNLFISLLNFFLLINLMNLIPNFFYISTNIIFTLNFSFWFINNFFIFNLNNNMNIFFMN
cox3	3079	3831	+	Single ORF	MNLNNFYFNIKISPWPIMISINMMNMMFNLILFLNFKFNMMMIIIILLINFNTMMLWINHMYLINFKMNYYNNFIKLTKKIFLMLFILSEMMFFLSFFYINFSIYYFNNIMFNFNNLNMI
nad3	3919	4218	+	Single ORF	MMNIFLIISLIMLMINKLNLKMKNNNFMNNIECGFNNMNNKHIPIYNNFFMIMIIFLIFDLEFFLLIPLILLFNKLNWLKLMMMMLIIFYLFFFIMWN
nad5.4	4895	5236	-	+1 frameshift at position 5170	MLLMYMYLYFFFFYSKINYNSYIFYIFFYFKDLFMEYFFMMYMNNFFFFFSMIYMMKIFLNLLLTNSMLVYYMNNKDLNYFNLILFFMLFLNIFLMKYLFKLYFFLIYVFFLV
nad5.3	5193	5591	-	+1 frameshift at position 5213	MVAPMPVSSLVHSSTLVVVGLYFLFRFSSFINLNILFYLSMLTLLFFGYNMIVSMDFKKIMALSTMNHMSLMMFFIYMKMNLYMYMYMMIHALFKSMIFMCIGVMIYFNFDIQDIRK
nad5.2	5724	5933	-	Unknown	MIFFNYLMLLFVFIMLFLIFSLNLFSMLIWWDLLGLVSFLLVLFYKSNKIINFSLIVMLLNRLSDFLYY*
nad5.1	5948	6085	-	Unknown	MNKNIMLTYLFLNFNYINFNLMFYFDKYNLFFMFILMMIFLMIFM*
nad4.3	6196	6495	-	-1 frameshift at position 6474	IFIYLMMFFFIFFVIYFNLNSPIMMGFISELFMMMFLYKFFYLLLFMIFFMFMINLMYNLKYFIYILFNYNNLMMLNNMIYMKFYMIFFLFYNKYFFYF*
nad4.2	6443	7057	-	-1 frameshift at position 7046	LFMYFFSYPLLMIVFNMDINLNLNLIYFLNFKLWVLLIFYLLFLVKMSLFIFHLWLIKVHVEVSIVNSVILSSLMLKIGSFMFLRFNLLINSNLFNLKVLIFSISFYGMILISLMNFLNFDIKLMIA
nad4.1	7011	7340	-	-1 frameshift at position 7046	IFFMLLFFFVDYLSWIFIILILIIFYMIFLFNIEYFNNKYLINLFFLCLNMIMLFIYNNLFILFLIYEMMMIFILFLINMFSYQFERLNSSMILFVYMFFFLSFINNCF*
nad4L	7479	7685	-	Single ORF	MNNKNILYMMILLEYLMMMYMYMFMYVYMYMYMYLYMYMYMYMLISLLESLLIMCFLIKMMYFLVMIM
nad6	7985	8299	+	Single ORF	MSKFNFLSSIMLMFMFIMLNHYNFKLKMNFNLMKMILIMMNFNMIFYLNKLFKMKFNMIEYYMMMMMNKNNYFNYFNLMIYLILIIMFMINFIMLKTYFPMRKI
cytb	8301	9392	+	Single ORF	MIKSLNIKTPSNLYFWWNFGSLISIYMMIQILFGFMLSMNYMILNNPFMSSFFIYYNINFGWLMRLTHSNLTSLIFLLIMIHIKRNILFNTYFNKMMWMSGMMMLIIFMLIAFLGYSLIV
nad1.4	9697	9849	-	Unknown	MFFSVNIMKISFYLILILIMILILFFRGCLVRFRMDKMLFLLWKLFSFNS
nad1.3	9825	10031	-	Unknown	MLKFLMWLISILVELNRIPFDFLESESELISGMNLEFSSLNFMIFFNWMFSYNFFKYFNFMFFLELML*
nad1.2	9919	10230	-	Unknown	MSFYFFLMVWSLNSIYIILSVIRLIIQNLSFEILFMMILFSLIILMKNFNLMFLNELNMISMIFFQNIKIFNMINFYFSWIKSYSIWFFSESISINFWNEFSI*
nad1.1	10227	10550	-	Unknown	MKIILILLMNMLSVGFYTLLEQKVLGYMNNRLGPNKIMILGVIQFMMDLIKLMFKDNIYLLMLNYLSFYVFILMFFSLSMFMWILMPFLINLMNFKFFMIFFSNYSK
Gene					**Amino acid sequence after frame shifts**
COX1					MYSTNHKNISLMYLLFGFWSGLMGLSMSFIIRIELMNLNNNFNNNMIYYMMITIHAFIMIFFMTMPIIIGSLSNWLLPLMLMSSDLIFPRLNNFSFWLLIPSLILMMMNMMLSNNINT
NAD4					MFFMLLFFFVDYLSWIFIILILIIFYMIFLFNIEYFNNKYLINLFFLCLNMIMLFIYNNLFILFLIYEMMMIFILFLINMFSYQFERLNSSMILFVYMFFSYPLLMIVFNMDINLNLNLIYFLNFKL
NAD5.3-4					MVAPMPVSSLVHSSTLVVVGLYFLFRFSSFINLNILFYLSMLTLLFFGYNMIVSMDFKKIMALSTMNHMSLMMFFIYMKMNLYMYMYMMIHALFKSMIFMCIGVMIYFNFDIQDIRK

See file Supp.table1.xlsx **for Table S1.**

Table S2. Proteomics Discoverer output

Supplementary table 2 Proteomics Discoverer output

Protein FDR	Genome	Description	Exp. q-value	Sum PEP Sco	Coverage [%	# Peptides	# PSMs	# Unique Pe	# AAs	MW [kDa]	calc. pI	Score Seque	# Peptides (t	# Protein Groups
High	Mitochondria	Mitochondria-COX2	0	43.037	31	6	13	6	221	26.7	8.35	35.11	6	1
High	Mitochondria	Mitochondria-COX3	0	22.659	13	3	5	3	250	30.9	9.45	12.69	3	1
High	Mitochondria	Mitochondria-COX1.2	0	8.689	13	1	3	1	190	22.5	9.47	9.35	1	1
High	Mitochondria	Mitochondria-ND3	0	7.599	16	1	3	1	110	13.6	9.6	3.82	1	1
High	Mitochondria	Mitochondria-ND4.2	0.001	3.095	4	1	1	1	202	24.5	9.57	2.4	1	1
High	Mitochondria	Mitochondria-ND1.1	0.001	2.745	7	1	1	1	109	13.2	9.66	1.8	1	1
High	Mitochondria	Mitochondria-CYTB	0.001	3.279	3	1	1	1	363	43.9	9.69	1.76	1	1
High	Moranella	Moranella-groL-chaperonin-GroEL	0	241.719	65	40	55	34	546	57.4	5.11	169.94	40	1
High	Moranella	Moranella-dnaK-molecular-chaperone DnaK	0	108.79	37	21	30	18	632	69.3	5.16	72.09	21	1
High	Moranella	Moranella-unknown-peroxiredoxin-C	0	49.253	63	12	15	11	200	22.6	7.97	28.74	12	1
High	Moranella	Moranella-tuf-elongation-factor Tu	0	55.973	35	11	11	11	394	43.2	5.69	24.9	11	1
High	Moranella	Moranella-pyk-pyruvate-kinase	0	47.171	26	9	9	9	480	51.6	6.48	21.09	9	1
High	Moranella	Moranella-ibpA-small-heat shock chaperone IbpA	0	29.689	59	6	6	6	138	15.5	5.87	19.34	6	1
High	Moranella	Moranella-eno-phosphopyruvate-hydratase	0	17.31	11	4	5	3	431	45.7	6.21	12.28	4	1
High	Moranella	Moranella-unknown-DNA-directed-RNA polymerase subunit alpha	0	23.11	16	3	4	3	329	36.4	5.5	11.17	3	1
High	Moranella	Moranella-rho-transcription-termination factor Rho	0	9.792	8	3	3	3	419	47	7.17	2.15	3	1
High	Moranella	Moranella-pnp-polyribonucleotide-nucleotidyltransferase	0	9.904	4	3	3	3	697	75.9	5.67	4.35	3	1
High	Moranella	Moranella-unknown-co-chaperone-GroES	0	15.742	39	3	3	3	97	10.3	6.11	9.96	3	1
High	Moranella	Moranella-ibpB-small-heat shock chaperone IbpB	0	13.318	14	3	3	3	159	18.1	6.09	7.73	3	1
High	Moranella	Moranella-gap-type-I glyceraldehyde-3-phosphate dehydrogenase	0	4.48	7	2	2	2	334	36	7.15	0	2	1
High	Moranella	Moranella-aceF-dihydrolipoyllysine-residue-acetyltransferase	0	8.621	6	2	2	2	424	46.7	5.91	3.07	2	1
High	Moranella	Moranella-unknown-single-stranded-DNA-binding protein	0	9.878	13	2	2	2	186	20.6	6.54	5.43	2	1
High	Moranella	Moranella-rpoC-DNA-directed-RNA polymerase subunit beta'	0	5.734	1	2	2	2	1402	155.6	7.11	0	2	1
High	Moranella	Moranella-rpsC-30S-ribosomal protein S3	0	6.935	9	2	2	2	232	26	10.32	2.79	2	1
High	Moranella	Moranella-hflK-FtsH-protease activity modulator HflK	0	7.622	3	1	1	1	405	45.4	9.04	2.82	1	1
High	Moranella	Moranella-grpE-nucleotide-exchange factor GrpE	0.001	3.345	7	1	1	1	199	22.5	4.82	0	1	1
High	Moranella	Moranella-rpsA-30S-ribosomal protein S1	0	4.012	3	1	1	1	556	61.2	5.86	0	1	1
High	Moranella	Moranella-rplE-50S-ribosomal protein L5	0	11.616	12	1	1	1	179	20.3	9.91	4.42	1	1
High	Moranella	Moranella-rpoB-DNA-directed-RNA polymerase subunit beta	0	8.906	2	1	1	1	1342	150.7	5.48	3.32	1	1
High	Moranella	Moranella-hflC-protease-modulator HflC	0	4.094	5	1	1	1	329	37.1	6.43	1.98	1	1
High	Moranella	Moranella-rdgC-recombination-associated-protein RdgC	0.001	3.162	5	1	1	1	301	33.7	8.29	2.47	1	1
High	Nuclear	Nuclear-pyruvate-carboxylase, mitochondrial-like isoform X1	0	962.981	85	114	559	1	1203	132.4	6.47	1560.16	114	1
High	Nuclear	Nuclear-pyruvate-carboxylase, mitochondrial-like isoform X1	0	955.718	85	112	556	1	1203	132.5	6.65	1553	112	1
High	Nuclear	Nuclear-ATP-synthase subunit beta, mitochondrial	0	507.05	74	38	555	38	523	55.8	5.48	1778.98	38	1
High	Nuclear	Nuclear-pyruvate-carboxylase, mitochondrial-like isoform X2	0	897.05	84	109	553	2	1187	130.7	6.6	1527.59	109	1

See Supp.table2.xlsx file for Table S2.

Table S3. *P. citri* tRNAs with mitogenome location and sequence as well as corresponding MITOS2 prediction of the locus and closest BLAST hit to scale insect relative.

Mitogenome assembly coordinates			Final tRNA annotation			
Start	Stop	Strand	tRNA	Sequence	A/T_bias	Length
4245	4302	+	**AlaTGC**	TAGATAAATCTTATTATTTGCAATAATAAATTATAATAAATATTTAATTATATTATCTAA	0.92	60
4303	4361	+	**ArgTCG**	TATATAAACTAACTTTAATTTCGACTTAAAATTATGAATTAATTAAATTCATTATATAA	0.88	59
4371	4425	+	**AsnGTT**	TTAATTGAAATTAATATTACTGTTAATAATATAAAGAATTAAAACTCCAATTAAG	0.85	55
2290	2351	+	**AspGTC**	AAAAAAATAGTTAATAAATATAATATAACATTAATTTGTCAAATTAAAATAATTTTTTTTTA	0.94	62
4236	4293	-	**CysGCA**	AATTAAATATTTATTATAATTTATTATTGCAAATAATAAGATTTATCTAATTTAATT	0.93	57
13758	13813	-	**GlnTTG**	TTTATTTAAAATTAATTTTTTGAAAATTAATAAATTAGTTAATTCTAATAAATAAAA	0.95	57
4480	4537	+	**GluTTC**	ATTTTTATAGTTTAAAATAAAACATTATATTTTCAATATAAAAATTTATTTAAAAATA	0.95	58
3840	3896	+	**GlyTCC**	ATTTTATTAATATATAATTAAGTATATTTAATTTCCAATTAAAAAGATATATAAAATA	0.93	58
6104	6169	-	**HisGTG**	ATTTATATATTTTAAGAAAAAAATTAATTTGTGAAATTAAAAATAAATTTAATTATTTTATAAATA	0.95	66
13808	13872	+	**IleGAT**	AATAAAATGCCTGATTAAAGGATTACTTCGATAAAGTAAATTATATAATAAAATTATTTTTATTA	0.85	65
1511	1574	+	**LeuTAA**	ATTAATATGGCAGAATAATATGCATTGAATTTAAAATTCAAATATAAATTAAATTTTATTAATA	0.88	64
10551	10611	-	**LeuTAG**	GATATTTATAAAATTAAATTTAGAATTTAAATTATAATTTTATTTAAAAATTAAAATATTA	0.97	61
2238	2290	+	**LysTTT**	ATTTAGATAATATTAATCTTTTAAATTAATTTAGTTAAATTAACTTCTAAATA	0.91	53
13645	13706	+	**MetCAT**	AGAAAAATAAGCTAAAACAAGCTTTTGAACTCATAATTCAAATATAAATTATTTTTTTTTCTA	0.83	63
4526	4589	-	**PheGAA**	ATTTAAATAGTTAAAATTATAATATTATTTTGAAAAAATAAAGTTAATAAATTATTTTTAAATA	0.95	64
7777	7832	-	**ProTGG**	CAGTAAATAGTTTAATTAAAAATAATAATTTTGGATATTATAGATTAATTTACTGA	0.86	56
4423	4478	+	**SerTCT**	AAGATAAATATAAATTTAAGCTTCTAACTTAAAATAAAAATAAATTTTTTATCTTT	0.89	56
9415	9467	+	**SerTGA**	AAGTTATAAATATTTATTTTGAAAATAAATTAAGCATTATTAGCAATAACTTT	0.87	53
7724	7777	+	**ThrTGT**	AAATTTTTAGTTTAAATAAAACGTTGATTTTGTAAATCAAAAAAAGTAAAATTTA	0.87	55
14822	14881	+	**TrpTCA**	AAGATTTTAAGTTAAATAAATAAACTATTAATTTTCAAAATTAAAAATTTATAAATCTTA	0.92	60
13708	13760	-	**TyrGTA**	AAATAAATTAATAATAAATTGTAAATTTATTAAAGAATTAAATTCTTTATTTA	0.94	53
13708	13765	+	**ValTAC**	TAAATAAAGAATTTAATTCTTTAATAAATTTACAATTTATTATTAATTTATTTATTTAA	0.95	59
7779	7832	+	**trnX**	AGTAAATTAATCTATAATATCCAAAATTATTATTTTTAATTAAACTATTTACTG	0.87	54

Green backgrounds correspond to a match between the final tRNA annotation and the predicted tRNA identity

Red nucleotides are post-transcriptional additions that are not encoded in the mitogenome sequence

See Supp.table3.xls file for Table S3.

Table S4.

Complete P. citri tRNA reference database used for mapping. Bacillus control tRNA was only used in MSR-seq analyses.

Genome	Anicodon	ID	Sequence
Bacillus	IleGAT	control	GGGCCTGTAGCTCAGCTGGTTAGAGCGCACGCCTGATAAGCGTGAGGTCGGTGGTTCGAGTCCACTCAGGCCCACCA
Mitochonc	ProTGG	78	CAGTAAATAGTTTAATTAAAAATAATAATTTTGGATATTATAGATTAATTTACTGACCA
Mitochonc	UnkNNN	78	AGTAAATTAATCTATAATATCCAAAATTATTATTTTTAATTAAACTATTTACTGCCA
Mitochonc	ThrTGT	133	AAATTTTTAGTTTAAATAAAACGTTGATTTTGTAAATCAAAAAAAGTAAAATTTACCA
Mitochonc	HisGTG	1741	ATTTATATATTTTAAGAAAAAAATTAATTTGTGAAATTAAAAATAAATTTAATTATTTTATAAATACCA
Mitochonc	PheGAA	3321	ATTTAAATAGTTAAAATTATAATATTATTTTGAAAAAATAAAGTTAATAAATTATTTTTAAATACCA
Mitochonc	GluTTC	3373	ATTTTTATAGTTTAAAATAAAACATTATATTTTCAATATAAAAATTTATTTAAAAATACCA
Mitochonc	SerTCT	3432	AAGATAAATATAAATTTAAGCTTCTAACTTAAAATAAAAATAAATTTTTTATCTTTCCA
Mitochonc	AsnGTT	3485	TTAATTGAAATTAATATTACTGTTAATAATATAAAGAATTAAAACTCCAATTAAGCCA
Mitochonc	ArgTCG	3549	TATATAAACTAACTTTAATTTCGACTTAAAATTATGAATTAATTAAATTCATTATATAACCA
Mitochonc	CysGCA	3617	AATTAAATATTTATTATAATTTATTATTGCAAATAATAAGATTTATCTAATTTAATTCCA
Mitochonc	AlaTGC	3608	TAGATAAATCTTATTATTTGCAATAATAAATTATAATAAATATTTAATTATATTATCTAACCA
Mitochonc	GlyTCC	4014	ATTTTATTAATATATAATTAAGTATATTTAATTTCCAATTAAAAAGATATATAAAATACCA
Mitochonc	AspGTC	5559	AAAAAAATAGTTAATAAATATAATATAACATTAATTTGTCAAATTAAAATAATTTTTTTTTACCA
Mitochonc	LeuTAA	6336	ATTAATATGGCAGAATAATATGCATTGAATTTAAAATTCAAATATAAATTAAATTTTATTAATACCA
Mitochonc	TrpTCA	7939	AAGATTTTAAGTTAAATAAATAAACTATTAATTTTCAAAATTAAAAATTTATAAATCTTACCA
Mitochonc	GlnTTG	9007	TTTATTTAAAATTAATTTTTTGAAAATTAATAAATTAGTTAATTCTAATAAATAAAACCA
Mitochonc	IleGAT	8948	AATAAAATGCCTGATTAAAGGATTACTTCGATAAAGTAAATTATATAATAAAATTATTTTTATTACCA
Mitochonc	TyrGTA	9060	AAATAAATTAATAATAAATTGTAAATTTATTAAAGAATTAAATTCTTTATTTACCA
Mitochonc	ValTAC	9055	TAAATAAAGAATTTAATTCTTTAATAAATTTACAATTTATTATTAATTTATTTATTTAACCA
Mitochonc	MetCAT	9114	AGAAAAATAAGCTAAAACAAGCTTTTGAACTCATAATTCAAATATAAATTATTTTTTTTTCTACCA
Mitochonc	LeuTAG	12209	GATATTTATAAAATTAAATTTAGAATTTAAATTATAATTTTATTTAAAAATTAAAATATTACCA
Mitochonc	SerTGA	13353	AAGTTATAAATATTTATTTTGAAAATAAATTAAGCATTATTAGCAATAACTTTCCA
Mitochonc	LysTTT	5620	ATTTAGATAATATTAATCTTTTAAATTAATTTAGTTAAATTAACTTCTAAATACCA
Moranella	ArgCCG	712	ACGCCCGTAGCTCAGCTGGATAGAGCGCTGCCCTCCGGAGGCAGAAGTCTCAGGTTCGAATCCTGTCGGGCGTACCA
Moranella	HisGTG	713	GTGATTGTAGCTCAGTTGGTAGAGCCCTGGATTGTGATTCCAGTTGTCGTGGGTTCAAGTCCCATCAGTCACCCCA
Moranella	LeuCAG	662	GCGAAGGTGGCGGAATTGGTAGACGCGCTAGCTTCAGGTGTTAGTGTCTTACCGGACGTGAGGGTTCAAATCCCTCTCTTCGCACCA
Moranella	ProTGG	796	CGGCGAGTAGCGCAGCTTGGTAGCGCAACTGGTTTGGGACCAGTGGGTCAGAGGTTCAAATCCTCTCTCGCCGACCA
Moranella	ValGAC	806	GCGTCCGTAGCTCAGTTGGTTAGAGCACCACCTTGACATGGTGGGGGTCAGTGGTTCGATTCCACTCGGACGTACCA
Moranella	TrpCCA	781	AGGGGCGTAGTTCAATTGGTAGAGCACCGGTCTCCAAAACCGGTTGTTGGGAGTTCAAGTCTCTCCGCCCCTGCCA

See Supp.table4.xlsx file for Table S4

Table S5. Mapped YAMAT read counts in mitochondrial isolates, total insect, and mitoribosome libraries. Any reads that mapped equally well to two or more references were removed from counts.

Library	Mitochondria-AlaTGC-3608	Mitochondria-ArgTCG-3549	Mitochondria-AsnGTT-3485	Mitochondria-AspGTC-5559	Mitochondria-CysGCA-3617	Mitochondria-GlnTTG-9007
Mitochondrial_isolation_1	1300072	716872	1169530	347442	410749	292434
Mitochondrial_isolation_2	1125677	626743	1131057	415426	291249	259337
Mitochondrial_isolation_3	1657444	819231	1320668	733473	305851	346487
Mitoribosome_1	165215	90212	2369233	215127	18214	67235
Mitoribosome_2	94759	32712	2620135	134485	16057	88622
Mitoribosome_3	235524	121022	5806763	319839	52874	1538
Total_insect_1	116070	67845	95693	20965	22955	32516
Total_insect_2	125543	74333	97172	26597	55280	37340
Total_insect_3	125232	75428	86129	51226	19934	38775

See file Supp.table5.xlsx for Table S5.

Table S6. EdgeR results for mitochondrial YAMAT libraries vs total insect YAMAT libraries

tRNA	Genome	avgCPM	logFC	logCPM	F-statistic	PValue	FDR
Mitochondria-AspGTC-5559	Mitochondria	8626.1778	5.19827763	13.0744925	215.86515	1.18E-41	1.57E-39
Mitochondria-SerTCT-3432	Mitochondria	42019.4002	5.0164735	15.3587649	214.147938	2.21E-41	1.57E-39
Mitochondria-GlyTCC-4014	Mitochondria	18425.9839	5.01713252	14.1694475	211.997109	4.85E-41	1.99E-39
Mitochondria-IleGAT-8948	Mitochondria	51540.9869	4.97310665	15.6534302	211.604973	5.60E-41	1.99E-39
Mitochondria-TrpTCA-7939	Mitochondria	46773.9281	4.95601107	15.5134144	210.379258	8.77E-41	2.49E-39
Mitochondria-MetCAT-9114	Mitochondria	74515.0501	4.90194702	16.1852426	207.370539	2.65E-40	6.27E-39
Mitochondria-AsnGTT-3485	Mitochondria	21273.8422	4.92247462	14.3767872	206.476908	3.68E-40	7.47E-39
Mitochondria-GluTTC-3373	Mitochondria	15146.6146	4.92906836	13.8867	205.068602	6.19E-40	1.02E-38
Mitochondria-LeuTAA-6336	Mitochondria	33840.3645	4.87969979	15.046454	204.947742	6.47E-40	1.02E-38
Mitochondria-SerTGA-13353	Mitochondria	32937.2391	4.87194098	15.0074281	204.396203	7.93E-40	1.05E-38
Mitochondria-PheGAA-3321	Mitochondria	27354.1796	4.87750163	14.7394693	204.33966	8.10E-40	1.05E-38
Mitochondria-ThrTGT-133	Mitochondria	8712.75107	5.00510093	13.0888993	203.980441	9.25E-40	1.09E-38
Mitochondria-ProTGG-78	Mitochondria	11602.2896	4.83685018	13.5021113	196.706281	1.38E-38	1.51E-37
Mitochondria-AlaTGC-3608	Mitochondria	24104.9584	4.71452658	14.5570373	193.594014	4.42E-38	4.48E-37
Mitochondria-ValTAC-9055	Mitochondria	40908.386	4.64134389	15.3201061	189.997859	1.71E-37	1.62E-36
Mitochondria-HisGTG-1741	Mitochondria	2117.86828	5.34014577	11.0483431	185.595159	9.00E-37	7.99E-36
Mitochondria-LysTTT-5620	Mitochondria	18534.9984	4.57751294	14.1779576	184.094609	1.59E-36	1.33E-35
Mitochondria-ArgTCG-3549	Mitochondria	12844.9799	4.55612434	13.6489077	180.210828	6.97E-36	5.50E-35
Mitochondria-CysGCA-3617	Mitochondria	6039.69139	4.64774554	12.5602381	173.45061	9.31E-35	6.96E-34
Mitochondria-LeuTAG-12209	Mitochondria	11969.0572	4.40190699	13.5470121	170.123712	3.37E-34	2.39E-33
Mitochondria-UnkNNN-78	Mitochondria	4815.05449	4.6042121	12.2333107	164.736868	2.73E-33	1.84E-32
Mitochondria-TyrGTA-9060	Mitochondria	7298.01003	4.28668637	12.8332708	157.37248	4.89E-32	3.16E-31
Mitochondria-GlnTTG-9007	Mitochondria	5373.00256	4.29569066	12.3914914	150.375799	7.81E-31	4.82E-30
Moranella-LysTTT-835	Moranella	787.618498	-2.0841153	9.62157569	33.4015034	1.24E-08	7.21E-08
Moranella-AlaTGC-735	Moranella	1831.88189	-1.965209	10.8392042	33.3470539	1.27E-08	7.21E-08
Moranella-LeuCAG-662	Moranella	651.016414	-2.0122542	9.3468192	30.8513487	4.28E-08	2.34E-07
Moranella-ThrGGT-762	Moranella	347.153753	-2.0190449	8.43990812	29.6826759	7.59E-08	3.99E-07
Moranella-AlaGGC-800	Moranella	417.574469	-1.9996556	8.70630145	29.5319812	8.17E-08	4.14E-07
Moranella-ValTAC-777	Moranella	1842.73851	-1.8006693	10.8477294	28.3187437	1.48E-07	7.26E-07
Moranella-PheGAA-797	Moranella	631.137279	-1.9218137	9.30207346	28.2477491	1.54E-07	7.27E-07
Moranella-IleGAT-691	Moranella	1976.09912	-1.7213223	10.9485183	26.2176254	4.18E-07	1.92E-06
Moranella-ValGAC-806	Moranella	327.005358	-1.8106306	8.35369422	24.1056345	1.19E-06	5.30E-06
Moranella-GlyTCC-696	Moranella	2539.95752	-1.6045078	11.3106445	23.6148023	1.52E-06	6.56E-06
Moranella-Ile2CAT-768	Moranella	301.463919	-1.7711884	8.23637168	22.9961082	2.08E-06	8.67E-06

See file Supp.table6.xlsx for Table S6.

Table S7. Sequencing matches and mismatches for all tRNAs, all positions for mitochondrial isolation YAMAT librarys

tRNA	Position	Reference	Match	Mismatch	A	C	G	T	Del	Ins	N
Mitochondria	1	T	1439347	15867	210	265	55	0	15337	17239	
Mitochondria	2	A	1443754	11460	0	21	299	354	10786	0	
Mitochondria	3	G	1443800	11414	246	79	0	2257	8832	0	
Mitochondria	4	A	1445469	9745	0	41	322	932	8450	11	
Mitochondria	5	T	1451861	3353	704	170	1893	0	586	76	
Mitochondria	6	A	1219610	235604	0	339	6373	919	227973	331	
Mitochondria	7	A	1310160	145054	0	462	38997	29613	75982	401	
Mitochondria	8	A	386936	1068278	0	28687	357970	681546	75	1765	
Mitochondria	9	T	1454197	1017	11	908	12	0	86	16078	
Mitochondria	10	C	1454484	730	146	0	1	557	26	44	
Mitochondria	11	T	1454183	1031	22	653	8	0	348	18	
Mitochondria	12	T	1453888	1326	801	464	23	0	38	441	
Mitochondria	13	A	1454379	835	0	300	113	240	182	8	
Mitochondria	14	T	1453522	1692	198	145	10	0	1339	53	
Mitochondria	15	T	1454838	376	143	173	24	0	36	194	
Mitochondria	16	A	1454959	255	0	6	118	105	26	11	
Mitochondria	17	T	1454529	685	49	187	29	0	420	327	
Mitochondria	18	T	1454862	352	14	272	33	0	33	58	
Mitochondria	19	T	1454837	377	30	290	43	0	14	4	
Mitochondria	20	G	1454734	480	276	60	0	54	90	15	
Mitochondria	21	C	1454605	609	41	0	22	444	102	29	
Mitochondria	22	A	1448427	6787	0	61	1334	2364	3028	278	
Mitochondria	23	A	1453150	2064	0	2	126	267	1669	54	
Mitochondria	24	T	1452658	2556	256	279	13	0	2008	4	
Mitochondria	25	A	1454863	351	0	5	152	22	172	272	
Mitochondria	26	A	1454899	315	0	9	138	38	130	9	
Mitochondria	27	T	1454695	519	108	129	110	0	172	44	
Mitochondria	28	A	1454373	841	0	6	152	92	591	650	
Mitochondria	29	A	1454769	445	0	6	187	117	135	22	
Mitochondria	30	A	1454629	585	0	13	178	263	131	110	

See file Supp.table7.xlsx for Table S7.

Table S8A-C. All MSR-seq counts for reads ending in CCA, CC or other: Average CCA containing reads per tRNA reference in all libraries: Aminoacylation-dependent protection of mitochondrial tRNAs relative to an uncharged spike-in. Effect sizes (odds ratios), confidence intervals, and FDR-corrected p-values from a binomial GLM normalized to untreated baseline levels.

tRNA	Treatment	Mean percentage of reads ending in CCA
Bacillus-IleGAT-control	Control	89.93
Bacillus-IleGAT-control	Periodate	1.98
Mitochondria-AlaTGC-3608	Control	67.79
Mitochondria-AlaTGC-3608	Periodate	19.05
Mitochondria-ArgTCG-3549	Control	74.26
Mitochondria-ArgTCG-3549	Periodate	49.93
Mitochondria-AsnGTT-3485	Control	81.59
Mitochondria-AsnGTT-3485	Periodate	39.76
Mitochondria-AspGTC-5559	Control	79.32
Mitochondria-AspGTC-5559	Periodate	45.52
Mitochondria-CysGCA-3617	Control	87.73
Mitochondria-CysGCA-3617	Periodate	25.49
Mitochondria-GlnTTG-9007	Control	95.33
Mitochondria-GlnTTG-9007	Periodate	57.43
Mitochondria-GluTTC-3373	Control	82.76
Mitochondria-GluTTC-3373	Periodate	42.72
Mitochondria-GlyTCC-4014	Control	83.37
Mitochondria-GlyTCC-4014	Periodate	47.80
Mitochondria-HisGTG-1741	Control	79.78
Mitochondria-HisGTG-1741	Periodate	44.98
Mitochondria-IleGAT-8948	Control	74.38
Mitochondria-IleGAT-8948	Periodate	18.05
Mitochondria-LeuTAG-12209	Control	55.32
Mitochondria-LeuTAG-12209	Periodate	34.09
Mitochondria-LeuTAA-6336	Control	73.55
Mitochondria-LeuTAA-6336	Periodate	24.73
Mitochondria-LysTTT-5620	Control	83.65
Mitochondria-LysTTT-5620	Periodate	51.42
Mitochondria-MetCAT-9114	Control	47.83

See file Supp.table8.xlsx for Table S8.

Table S9 A-B. YAMAT-seq adapters and primers: primers for RT-qPCR of rRNA

Name	Sequence
YAMAT_5-AD-A	GTTCAGAGTTCTACAGTCCGACGATCACTGGATACTGrGrA
YAMAT_5-AD-G	GTTCAGAGTTCTACAGTCCGACGATCACTGGATACTGrGrG
YAMAT_5-AD-C	GTTCAGAGTTCTACAGTCCGACGATCACTGGATACTGrGrC
YAMAT_5-AD-U	GTTCAGAGTTCTACAGTCCGACGATCACTGGATACTGrGrU
YAMAT_3-AD	/5Phos/GTATCCAGTTGGAATTCTCGGGTGCCAAGG/3ddC/
YAMAT_RT	GCCTTGGCACCCGAGAATTCCA
YAMAT_PCR_F	AATGATACGGCGACCACCGAGATCTACACGTTCAGAGTTCTACAGTCCGA
YAMAT_PCR_F	CAAGCAGAAGACGGCATACGAGATCGTGATGTGACTGGAGTTCCTTGGCACCCGAGAATTCCA
YAMAT_PCR_F	CAAGCAGAAGACGGCATACGAGATACATCGGTGACTGGAGTTCCTTGGCACCCGAGAATTCCA
YAMAT_PCR_F	CAAGCAGAAGACGGCATACGAGATGCCTAAGTGACTGGAGTTCCTTGGCACCCGAGAATTCCA
YAMAT_PCR_F	CAAGCAGAAGACGGCATACGAGATTGGTCAGTGACTGGAGTTCCTTGGCACCCGAGAATTCCA
YAMAT_PCR_F	CAAGCAGAAGACGGCATACGAGATCACTGTGTGACTGGAGTTCCTTGGCACCCGAGAATTCCA
YAMAT_PCR_F	CAAGCAGAAGACGGCATACGAGATATTGGCGTGACTGGAGTTCCTTGGCACCCGAGAATTCCA

See file Supp.table9.xlsx for Table S9.

Table S10. Genbank locus IDs for AlaRS, CysRS, TyrRS, and ValRS

aaRS	Genbank locus accession numbers
AlaRS	XP_065202421
CysRS	XP_065225826
TyrRS	TyrRS: XP_065210105/ XP_065210096
ValRS	XP_065200889

SI References

Darty K, Denise A, Ponty Y. 2009. VARNA: Interactive drawing and editing of the RNA secondary structure. Bioinformatics 25:1974–1975.